


Spring 5-11-2018

Polyp to Population: A Tale of Two Corals

Christopher T. Fountain

University of Maine, c.tyler.fountain@gmail.com

Follow this and additional works at: <https://digitalcommons.library.umaine.edu/etd>

 Part of the [Environmental Health and Protection Commons](#), [Marine Biology Commons](#), and the [Population Biology Commons](#)

Recommended Citation

Fountain, Christopher T., "Polyp to Population: A Tale of Two Corals" (2018). *Electronic Theses and Dissertations*. 2856.
<https://digitalcommons.library.umaine.edu/etd/2856>

This Open-Access Thesis is brought to you for free and open access by DigitalCommons@UMaine. It has been accepted for inclusion in Electronic Theses and Dissertations by an authorized administrator of DigitalCommons@UMaine. For more information, please contact um.library.technical.services@maine.edu.

POLYP TO POPULATION: A TALE OF TWO CORALS

By

C. Tyler Fountain

B. A. Capital University, 2013

A Thesis

Submitted in Partial Fulfillment of the

Requirements for the Degree of

Master of Science

(in Marine Biology)

The Graduate School

The University of Maine

May 2018

Advisory Committee:

Dr. Rhian Waller, Associate Professor of Marine Science, Advisor

Dr. Peter Auster, Research Professor Emeritus of Marine Science, University of Connecticut

Dr. Robert Steneck, Professor of Oceanography, Marine Biology, and Marine Policy

POLYP TO POPULATION: A TALE OF TWO CORALS

By C. Tyler Fountain

Thesis Advisor: Dr. Rhian Waller

An Abstract of the Thesis Presented
in Partial Fulfillment of the Requirements for the
Degree of Master of Science
(in Marine Biology)

May 2018

Deep-sea corals are of conservation concern in the North Atlantic due to prolonged disturbances associated with the exploitation of natural resources and a changing environment. As a result, the recovery rates of deep-sea coral communities are of heightened interest. These recovery rates are suggested to be on the order of decades to millennia, based on slow growth rates and longevity, of various deep-sea coral species. In 2014 and 2017 two research cruises in the Gulf of Maine, collected samples of two locally dominant species, *Primnoa resedaeformis* and *Paramuricea placomus*. These specimen collections were coupled with video surveys, conducted by remotely operated vehicles (ROVs), and used in conjunction with paraffin histologic technique. This study established an understanding of regional scale gametogenic variability between coral subpopulations within the Gulf of Maine. By investigating relationships between morphology and reproduction, this study also provides the data necessary for quantifying whole colony reproductive potentials and estimating population scale reproductive potentials. This will allow for future survey work to use colony heights as a proxy measurement for estimating the reproductive output of these coral habitats. In addition, previously published data on growth rates provided a means of calculating the size of first reproduction in these species. These data strengthen our fundamental understanding of the reproductive ecology of deep-sea corals, and will help to further identify key source populations to protect and mitigate future damage and thus facilitate recovery.

DEDICATION

*In memory of Peri Fountain,
whose abbreviated yet impactful life
is a reminder to face every day
with ferocity and passion.*

ACKNOWLEDGEMENTS

I would like to thank my advisor, Dr. Rhian Waller, in addition to my committee members, Dr. Peter Auster and Dr. Robert Steneck, for their guidance, patience, and sage advice. I would also like to thank our scientific collaborators, at NOAA and USGS, Dr. Martha Nizinski, Dave Packer, and Dr. Cheryl Morrison, for sample collection and geographic visualization. This work was funded by the National Oceanic and Atmospheric Administration's Deep Sea Coral Research and Technology Program through NOAA Contracts EA-133F-14-SE-3060 all to the University of Connecticut and NOAA Grant NA14OAR4320158 through the Cooperative Institute for North Atlantic Region to the University of Maine.

A special shout out goes to my lab mates: Ashley Rossin, Julia Johnstone, Elise Hartill, Lauren Rice, Isabelle Landers Holt, Gus Pendleton, Genny Wilson, Diego Gamero Huayhua, Jen Field, and Keri Conley for helping to refine my understanding of histology; and Dr. Robert Boenish for help with modeling work. In addition, I would like to thank the faculty and staff of the University of Maine's School of Marine Science and the fantastic cohort of students that I have been fortunate to work with. Thank you Mom, thank you Dad, thank you Tillie, and thank you Tad for your support along this journey.

TABLE OF CONTENTS

DEDICATION ii

ACKNOWLEDGEMENTS iii

LIST OF TABLES vi

LIST OF FIGURES vii

LIST OF EQUATIONS ix

Chapter

1. THE REPRODUCTIVE ECOLOGY OF *PRIMNOA RESEDAEFORMIS* AND
PARAMURICEA PLACOMUS, TWO DEEP-SEA CORALS LOCAL TO THE
GULF OF MAINE 1

Introduction 1

Methods 6

 Histology 8

 Video Analysis 10

Results 11

 Characterizing Gametogenesis 11

 Spermatogenesis 14

 Oocyte Diameter and Height Distribution 15

 Differences Among Subpopulations 17

 Seasonal Reproductive Variability 20

 Fecundity 21

 Morphometric Regression Analyses 23

 Size and Age at Maturation 28

Modelling Reproductive Potential	30
Discussion	36
Conclusion	40
Epilogue.....	42
REFERENCES	43
APPENDIX. ADDITIONAL FIGURES AND DATA FROM 2017 CRUISE.....	48
BIOGRAPHY OF THE AUTHOR.....	49

LIST OF TABLES

Table 1.	Sample collections by location and year.....	6
Table 2.	Descriptive statistics summarizing the data in Figure 6	17
Table 3.	<i>P. placomus</i> : Range in reproductive maturation expressed as size and time	28
Table 4.	<i>P. resedaeformis</i> : Range in reproductive maturation expressed as size and time.....	29
Table 5.	<i>P. placomus</i> : Estimated total potential fecundity, proportion vitellogenic oocytes, and age based on mean heights from sample locations	33
Table 6.	<i>P. resedaeformis</i> : Estimated total colony fecundities and proportion vitellogenic oocytes, and age based on mean heights from each sample location.....	34

LIST OF FIGURES

Figure 1.	Map plate showing sample locations from 2014 and 2017 in addition to bathymetric maps from 2014	7
Figure 2.	Morphometric data collection from a <i>P. placomus</i> colony using the image analysis software Image J.....	10
Figure 3.	Example of the differentiation between vitellogenic and previtellogenic oocytes	12
Figure 4.	The stages of spermatogenesis in <i>P. resedaeformis</i> and <i>P. placomus</i>	13
Figure 5.	Developmental distribution of spermatocysts based staging scheme	15
Figure 6.	Histograms showing the frequency distribution of oocyte feret diameters and colony heights, between <i>P. placomus</i> (left) and <i>P. resedaeformis</i> (right)	16
Figure 7.	<i>P. placomus</i> , Histograms showing the difference in oocyte diameter (left) and colony height (right) distributions between 2014 sampling locations	17
Figure 8.	Histograms showing the difference in <i>P. resedaeformis</i> oocyte diameter (left) and colony height (right) distributions between 2014 sampling locations	19
Figure 9.	Comparison of oocyte diameters between August 2014 and June 2017 among both <i>P. placomus</i> (Top) and <i>P. resedaeformis</i> (Bottom)	20
Figure 10.	Boxplots of the fecundity distributions between sampling locations	22
Figure 11.	Regression analysis providing the mathematical relationship between height and fecundity of <i>P. placomus</i>	23

Figure 12. Regression analysis, of <i>P. placomus</i> , providing the mathematical relationship between height and polyps per axial cm	23
Figure 13. Using HD video analysis 59 individual colonies of <i>P. placomus</i> were analyzed and an exponential regression was used to develop a functional relationship between colony height and Total Branch Length (TBL)	25
Figure 14. Regression analysis providing the mathematical relationship between height and fecundity of <i>P. resedaeformis</i>	27
Figure 15. Regression analysis, of <i>P. resedaeformis</i> , providing the mathematical relationship between height and polyps per axial cm	27
Figure 16. Modeled relationships between colony fecundity and height/age	32
Figure 17. Height distribution frequencies, of <i>P. placomus</i> , by sampling location, plotted on top of the total fecundity (black) and proportion vitellogenic oocytes (blue) models	33
Figure 18. Calculated age distribution frequencies, of <i>P. resedaeformis</i> , by sampling location, plotted on top of the total fecundity (black) and proportion vitellogenic oocytes (blue) models	34
Figure 19. Oocyte size distribution of <i>P. placomus</i> from samples collected in June 2017 from the Western Jordan Basin (WJB)	48
Figure 20. Oocyte size distribution of <i>P. resedaeformis</i> from samples collected in June 2017 from the Western Jordan Basin (WJB), Nygren-Heezen InterCanyon (NHI), and Corsair Canyon (CC).....	48

LIST OF EQUATIONS

Equation 1. Feret Diameter	9
Equation 2. <i>Primnoa resedaeformis</i> : Functional Relationship Between Height and Age (Mortensen and Buhl-Mortensen 2005)	29
Equation 3. <i>Primnoa resedaeformis</i> : Functional Relationship Between Height and Age (Mortensen and Buhl-Mortensen 2005)	29
Equation 4. The Master Equation.....	30
Equation 5. <i>Paramuricea placomus</i> : Functional Relationship Between Fecundity and Colony Height	31
Equation 6. <i>Paramuricea placomus</i> : Functional Relationship Between Polyps per Axial Centimeter and Colony Height	31
Equation 7. <i>Paramuricea placomus</i> : Functional Relationship Between Total Branch Length and Colony Height.....	31
Equation 8. <i>Paramuricea placomus</i> : Total Colony Fecundity as a Function of Colony Height.....	31
Equation 9. <i>Paramuricea placomus</i> : Effective Relative Colony Fecundity as a Function of Colony Height	31
Equation 10. <i>Primnoa resedaeformis</i> : Functional Relationship Between Fecundity and Colony Height	31
Equation 11. <i>Primnoa resedaeformis</i> : Functional Relationship Between Polyps per Axial Centimeter and Colony Height	31
Equation 12. <i>Primnoa resedaeformis</i> : Functional Relationship Between Total Branch Length and Colony Height	31

Equation 13. *Primnoa resedaeformis*: Total Colony Fecundity as a Function of
Estimated Colony Age31

Equation 14. *Primnoa resedaeformis*: Effective Relative Colony Fecundity as a
Function of Estimated Colony Age.....31

CHAPTER 1

THE REPRODUCTIVE ECOLOGY OF *PRIMNOA RESEDAEFORMIS* AND *PARAMURICEA PLACOMUS*, TWO DEEP-SEA CORALS LOCAL TO THE GULF OF MAINE

Introduction

Deep-sea corals can function as foundation species and ecosystem engineers that serve as physical habitat used by a myriad of taxa, and are at high risk from select fishing practices, anthropogenic, and natural environmental variability. These structure-forming species increase the complexity of the environments in which they grow (Jones *et al* 1994; Lumsden *et al* 2007; Kahng *et al* 2011; Soetaert *et al* 2016). Classified in Jones *et al* (1994) as autogenic engineers, associated organisms rely on the physical growth of corals to change the environment by providing shelter, altering resource flows, and increasing niche availability (Metaxas and Davis 2005; Lacharite and Metaxas 2013; Soetaert *et al* 2016). Their branching morphology and considerable size, create space for other organisms to seek refuge, increase habitat variability, and result in more opportunity for increases in abundance of associated fauna and increases in faunal densities (Etnoyer and Morgan 2005; Lumsden *et al* 2007; Watanabe *et al* 2009; Cairns and Bayer 2009; Tong *et al* 2012; Lacharite and Metaxas 2013). Within the Northeast Channel and Gulf of Maine, 97 epifaunal species (Metaxas and Davis 2005), and various megafauna, including Acadian redfish, cusk, silver hake, Atlantic cod, and pandalid shrimp have been observed to associate with *P. resedaeformis* and *P. placomus* colonies (Personal observation; Auster 2005; Auster *et al* 2013; Auster *et al*

2014). *P. placomus* and *P. resedaeformis* exhibit two different growth forms commonly seen among octocorals. *P. resedaeformis*, with its arborescent growth, and *P. placomus*, with generally planar growth, display traits that classify them, according to Etnoyer and Morgan (2005), as habitat-forming organisms.

The growth and formation of deep-sea coral habitat occurs on the time-scale of decades to centuries, making them vulnerable to high impact disturbances such as bottom trawling, oil and gas exploration, and increased ocean stratification and acidification due to climate change (Lumsden *et al* 2007; Mercier and Hamel 2011; Soetaert *et al* 2016). As a means of gauging the amount of time required for habitat formation to occur, Andrews *et al* (2002) used ring count and radiometric data to quantify growth rates of *P. pacifica* (published as *P. resedaeformis*). This work was further validated by Sherwood *et al* (2005) by using ¹⁴C markers from atomic bomb testing to verify that banding (growth rings) of *P. resedaeformis* is annual.

Growth rates of gorgonians are primarily measured in two different ways, both axially and radially. Axial growth, which will be focused on later in this manuscript, is the elongation of the main stem and branches (Watling *et al* 2011). Comparatively, radial growth rates, often significantly slower and more discrete, are the thickening of axial components (Roberts *et al* 2009). Radial growth rates of *P. resedaeformis* are relatively constant over time as shown by a strong linear relationship between age and colony diameter (Mortensen and Buhl-Mortensen 2005). *P. resedaeformis* has an axial growth rate of 0.15 - 2.92 cm per year showing variation among geographic regions and with colony age (Andrews *et al* 2002; Risk *et al* 2002; Mortensen and Buhl-Mortensen 2005; Sherwood and Edinger 2009). Additionally, two *Paramuricea* specimens, collected from the

Central Labrador Slope, were estimated to have axial growth rates of 0.51 - 0.61 cm per year (Sherwood and Edinger 2009). *P. resedeaformis* colony size has been observed to range from 5 – 115cm (Mortensen and Buhl-Mortensen 2005; Pers Obs), and colony size of *P. placomus* has been observed to range from 5 – 65 cm (Pers Obs). These large maximum colony sizes and slow growth rates show that habitat formation and resultant ecological engineering functions occur over extensive periods of time, inferring that recovery may be on the scale of decades to centuries (Andrews *et al* 2002; Watling and Auster 2005; Waller *et al* 2007).

Communities formed by dense aggregations of one or more species of deep-sea octocorallians are known as “coral gardens” (ICES report 2007; Bullimore *et al* 2013). Minimum densities required for this classification of habitat are 0.1 colonies per m² (Bullimore *et al* 2013). However, this metric has proven difficult to use due to variations in colony densities, based on size and species composition (ICES report 2007). In addition to slow growth and habitat disturbance, part of the reason deep-sea coral conservation has been so difficult is due to uncertainties in species distribution (Watling and Auster 2005). These uncertainties have led to an increase in exploration studies and sampling of deep-sea corals, as well as supporting the development of higher resolution habitat suitability models used to predict and map spatial distributions (Bryan and Metaxas 2007; Yesson *et al* 2012). As an understanding of spatial distribution continues to resolve, the opportunity to facilitate more informed decisions to protect these ecosystems strengthens (van Hooidek *et al* 2016).

The distribution of deep-sea coral species is likely dependent upon locations where seawater temperature, current, depth, substrate composition and texture, slope and aspect are all suitable

(Sun *et al* 2010; Tong *et al* 2012). Consistencies in water temperature are important, particularly with octocorals as they are stenothermal (Buhl-Mortensen *et al* 2015). However, it is thought that reproductive processes may also be limiting population distributions (Lacharite and Metaxas 2013) indicating that areas with suitable substrate remain devoid of settlement. Two deep-sea octocorals found in the Gulf of Maine, *P. resedaeformis* and *Paragorgia arborea*, have shown preference towards hard substrates composed of cobbles, pebbles and boulders (Lacharite and Metaxas 2013) which provide sufficient stability for attachment as colonies continue to grow (Mortensen and Buhl-Mortensen 2005). Importantly, these deep-sea corals are sessile benthic suspension feeders that rely on the delivery of nutrients via advection to sustain metabolic processes (Soetaert *et al* 2016) such as growth and reproduction. *P. resedaeformis* is a known broadcast spawner relying on fertilization and development to happen in the water column (Kahng *et al* 2011; Mercier and Hamel 2011; Lacharite and Metaxas 2013). Broadcast spawning, a reproductive strategy seen among many coral species, maximizes fertilization rates while subsequently minimizing sperm limitation, and mitigates the effects of predation through over satiation (Alino and Coll 1989; Lasker *et al* 1996). The biophysical interaction between *P. resedaeformis* and localized hydrodynamics establishes a mechanism for population connectivity and increases the likelihood of larval dispersal (Sun *et al* 2010). Understanding population connectivity is noted as one of the greatest challenges to coral science; and regarding benthic suspension feeders, this challenge is often associated with the demographic linkage of local populations through the dispersal of larvae (Sale *et al* 2005; Jones *et al* 2009). Quantifying connectivity is important for the determination of natural and anthropogenic influences that limit growth and stability of populations, and thus allows for management at appropriate scales (Jones *et al* 2009). The motivation behind this study is in response to historical population impacts and environmental change. This study aims to provide

reproductive data used to inform connectivity models, while investigating local scale geographic differences in gamete development.

In 2014 and 2017, two research cruises in the Gulf of Maine collected samples of *P. resedaeformis* and *P. placomus*. These species of focus were based on their local dominance, high colony densities, and habitat reduction to potentially small refugia due to prolonged disturbance associated with select fishing practices (Watling and Auster 2005; Auster *et al* 2013). Specimen collections from 2014 were coupled with remotely operated vehicle (ROV) video surveys. Combined, these data were used to: characterize gametogenesis, evaluate oocyte size frequencies, discern reproductive and colony size differences among subpopulations, compare seasonal reproductive variability, quantify per polyp fecundity, assess morphometric and reproductive relationships, calculate size and age ranges at maturation, and develop individual based reproductive models. Investigating these biological elements provides insight into the potential reproductive output of entire coral colonies and a snapshot of gametogenic seasonality using techniques described in Waller *et al* (2014). These data are a critical aspect for strengthening the understanding of potential recovery rates and population resilience among deep-sea coral species and for identifying the most fecund source populations. The goal of this project is to combine size relative species fecundity and population size distributions to understand the potential whole population fecundity of these deep-sea coral species within the Gulf of Maine region. These estimations will help to further identify habitat areas of particular concern (HAPC) to protect and/or mitigate future damage. Protection of these habitat areas may prove to be invaluable investments for the future of deep-sea biodiversity in the Gulf of Maine.

Methods

Remotely Operated Vehicles, *Kraken II* (University of Connecticut) and *ROPOS* (Canadian Scientific Submersible Facility), were used to collect branches from two locally dominant deep-sea coral species, *P. resedaeformis* and *P. placomus*, during two research cruises within the Gulf of Maine (**Table 1**). From July 24th to August 4th, 2014 coral samples were collected from the Western Jordan Basin (WJB), Outer Schoodic Ridge (OSR), and Central Jordan Basin (CJB) onboard the R/V *Connecticut* (n=74, **Figure 1**). Additional samples were collected between June 12th and June 17th, 2017, from Western Jordan Basin (WJB), Nygren-Heezen InterCanyon (NHI), Corsair Canyon (CC), and George’s Canyon (GC) onboard the NOAA ship *Henry B. Bigelow* (n=35, **Figure 1**). Collections from 2017 aid in the reproductive biology study by increasing sample size, repeat sampling from WJB, and providing geographic contrast between the Gulf of Maine and proximate continental margin sites. All samples collected, once onboard, were fixed in 4% buffered formalin in preparation for laboratory analysis using histology.

Table 1. Sample collections by location and year.

Sample Area	July 24 th – August 4 th 2014		June 12 th – June 17 th 2017	
	Depth Range (m)	Samples Collected (n)	Depth Range (m)	Samples Collected (n)
Western Jordan Basin (WJB)	211 – 243	36	216 – 234	21
Central Jordan Basin (CJB)	206 – 214	12	-	-
Outer Schoodic Ridge (OSR)	167 – 212	26	-	-
Nygren-Heezen Inter Canyon (NHI)	-	-	667 – 771	7
Corsair Canyon (CC)	-	-	366 – 549	4
George’s Canyon (GC)	-	-	423 – 486	3

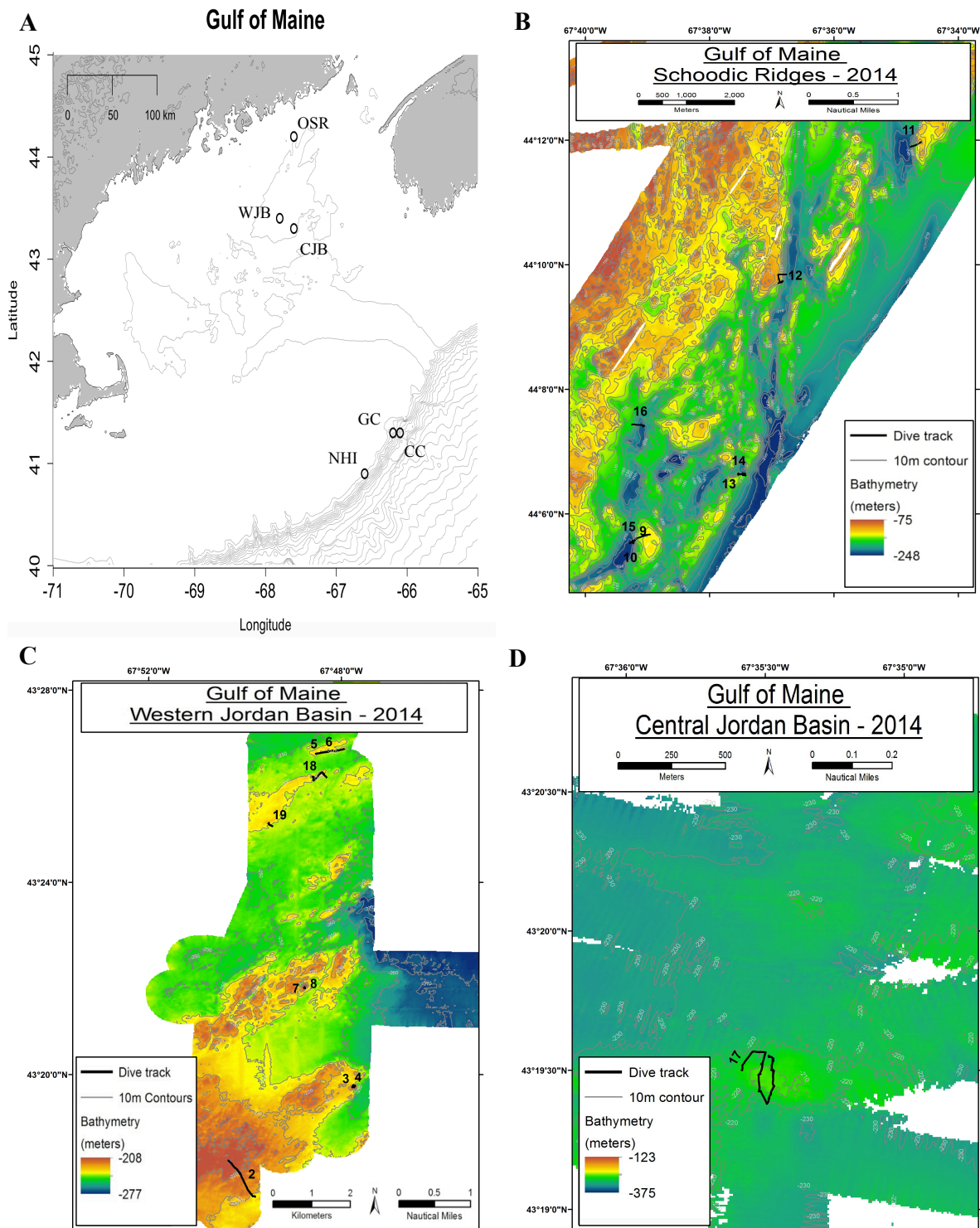


Figure 1. Map plate showing sample locations from 2014 and 2017 in addition to bathymetric maps from 2014. **A** Spatial distribution of sampling locations throughout the Gulf of Maine and marginal canyons, grey lines show 200m depth contours. **B-D** Bathymetric maps showing numbered ROV transects from Outer Schoodic Ridge (**B**) Western Jordan Basin (**C**) and Central Jordan Basin (**D**). Maps **B-D**, courtesy of Dave Packer, NOAA federal.

Histology

Coral samples were prepared following the methodology of Waller *et al* 2014, which worked with *Primnoa pacifica*, a sister species and morphologically similar to *P. resedaeformis*. Preparation of *Paramuricea placomus* deviated slightly due to the smaller size and fragility of samples although the same histologic protocol was followed. *P. resedaeformis* subsample preparation consisted of removing the central axis prior to the decalcification of spicules in Rapid Bone Decalcifier (American MasterTech Scientific). Similarly, *P. placomus* subsamples had their central axis dissected out and were then placed in Cal-Ex (Fisher Scientific) to dissolve the remaining calcareous components (sclerites). Once supporting structures were removed and decalcified, subsamples were dehydrated, over the course of 2.5-3.5 hours, through a series of ethanol baths; graded from 30%-100% following a 5%-10% increase between each step then left to sit in 100% ethanol overnight. The dehydration process of *P. resedaeformis* took place using a rotary mixer to eliminate internal tissue bubbles and *P. placomus* dehydration was carried out in a 500ml jar because bubble entrapment in tissue was negligible. Tissues were then rinsed in a final 100% ethanol bath before being cleared in Xylenes, a histologic clearing agent miscible in both ethanol and paraffin. Once cleared, the subsamples were placed into molten paraffin for up to 48 hours. This extended period of time ensured each tissue sample was completely infiltrated with paraffin before being embedded into standard histology molds for slicing using a MEDITE embedding station. Once the paraffin molds containing the tissue subsamples were hardened, they were sectioned using a MICROM HM325 or LEICA RM2155 microtome. Serial slicing occurred at 7 μ m (*P. resedaeformis*) or 5 μ m (*P. placomus*) increments based on nuclear diameters of oocytes.

Before starting sample analysis of fecundity and oocyte diameter, it was necessary to determine the oocyte nuclear diameters of each species. These measurements were obtained by initial histologic processing of each species and measuring the feret diameter of more than 100 random oocyte nuclei. The feret diameter was calculated from the area of the circled nucleus/oocyte as if it were a perfect circle (**Equation 1**). The average of the sampled nuclei, calculated nuclear diameter, was then subsequently used to measure out the distance of separation between sectioning while slicing paraffin blocks. This spacing, of one nuclear diameter, is necessary to reduce the possibility of double counting oocytes when quantifying fecundities per polyp, as only sections consisting of nucleus material were counted. Slides were stained using Masson's Trichrome and then viewed under an Olympus CX31 light microscope to count and photograph oocytes using infinity capture software (*Lumenera*), and spermatocysts were staged. Fecundity was determined by averaging the total number of oocytes per polyp across three randomly selected polyps from each female sample. While counting, oocytes were also categorized as either vitellogenic or previtellogenic, as a means of quantifying the proportion of viable oocytes per reproductive cohort. This oogenic distinction was made following descriptions from Fadlallah 1983, Waller and Tyler 2005, and Roberts *et al* 2009 (See below, in addition to **Figure 3**, results section). Feret diameter was then calculated from 100 randomly selected oocytes, photographed using a microscope mounted Infinity 1 camera (*Lumenera*), and circled using Image J (NIH), for determination of oocyte size distribution among species, individuals, and location.

Equation 1.
$$FeretDiameter = \frac{\sqrt{4 \times area}}{\pi}$$

Video Analysis

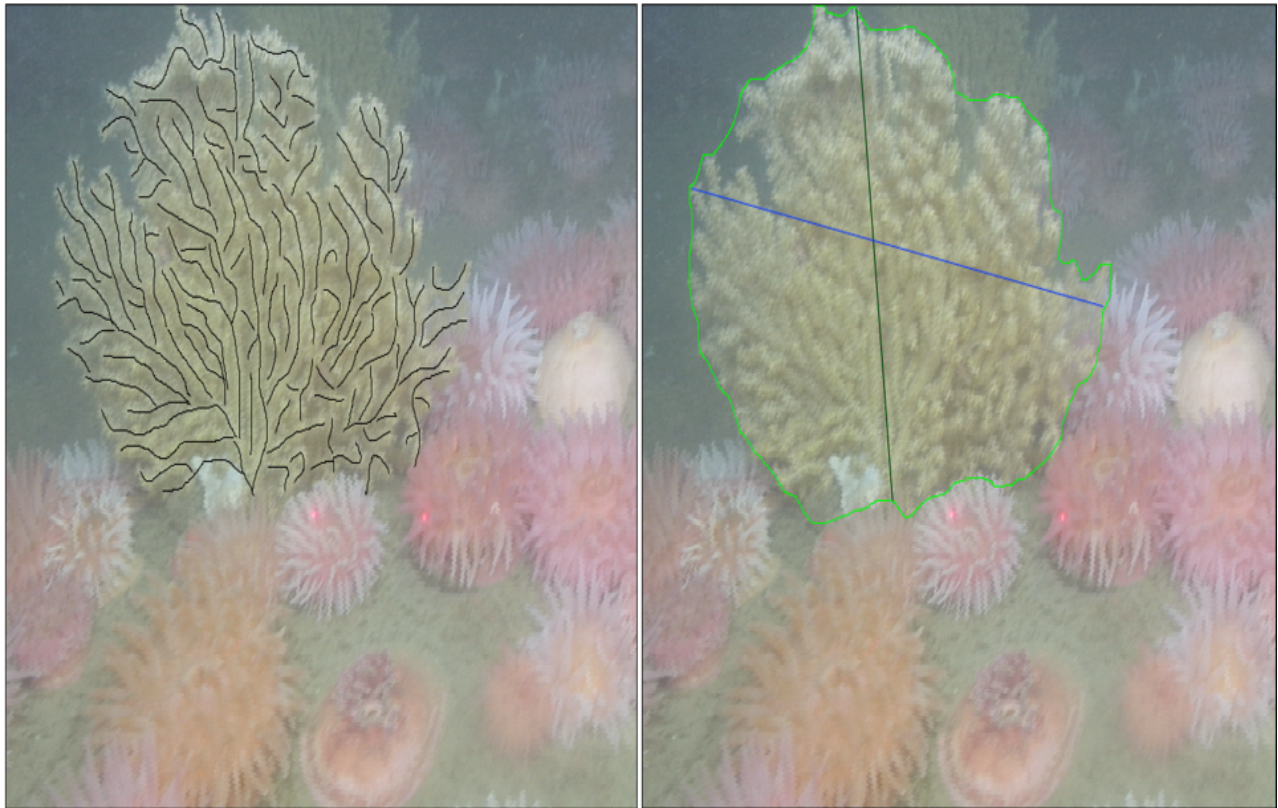


Figure 2. Morphometric data collection from a *P. placomus* colony using the image analysis software Image J. Photograph taken from ROV video transects. Laser calipers 10cm apart.

Video transects were taken coincident with sample collection dives in 2014 by the *Kraken* ROV. This video imagery was used to estimate coral colony morphometrics along ROV transects (**Figure 2**). Sizing of colonies is important because it can have a major influence on a colony's reproductive capacity, especially for organisms which may have genetically indeterminate growth, such as corals (Hall and Hughes, 1996). To obtain the most precise size estimate, the coral colony needed to be in plane with the video and paired parallel lasers (10 cm spacing; mounted on the video camera) projected as close as possible to the base of the colony for size scaling. Frame captures were then taken and colony morphometrics analyzed using Image J. Morphometrics collected were: height and total branch length. These metrics were then used as a means of developing size

distributions of coral colonies among the various sampling locations and in correlation analyses with reproductive data. Additional morphometric data, quantifying the number of polyps per axial cm, were collected using a Motic SMZ-168 dissecting scope, used to inform a colony based reproductive potential model.

Results

Characterizing Gametogenesis

Both species in this study are gonochoristic. Of the 55 *P. placomus* samples analyzed 21 were female, 25 were male, and 9 were non-reproductive individuals. This results in a 0.84:1, female to male ratio among colonies of *P. placomus*. Similarly, *P. resedaeformis* colonies exhibited a 0.85:1 ratio of females to males, based on measurements from 54 samples: 23 females, 27 males, and 3 non-reproductive individuals. However, of the *P. resedaeformis* samples examined, one was an aberrant hermaphrodite, which was exceptionally fecund and virile (Sample ID, OSR 100-1).

Female gametogenesis, examined quantitatively and seen in **Figure 3**, was used to investigate the proportion of vitellogenic to pre-vitellogenic oocytes present in collected specimens. This showed that 12% of the oocytes examined for *P. placomus* and 16% for *P. resedaeformis* were vitellogenic. These proportions are important to the “Modeling Reproductive Potential” section as they help quantify the effective relative fecundity (ERF). Described below are the criteria which constituted differentiation between previtellogenic and vitellogenic oocytes.

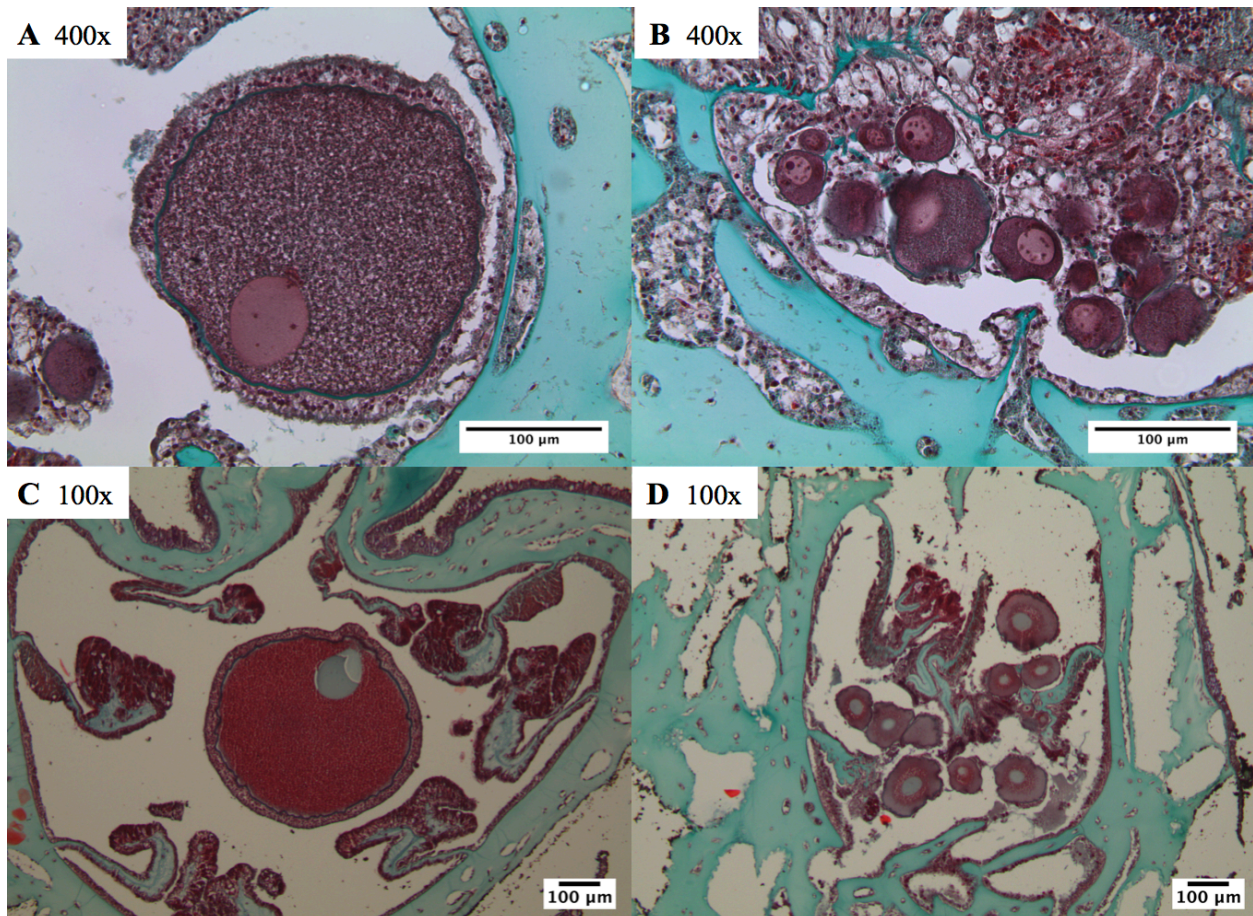


Figure 3. Example of the differentiation between vitellogenic and previtellogenic oocytes: **A** showing a well-developed vitellogenic oocyte of the species *P. placomus*, 400x magnification; **B** previtellogenic oocytes of the species *P. placomus*, 400x magnification; **C** vitellogenic oocyte of the species *P. resedaeformis*, 100x magnification; **D** A cluster of previtellogenic oocytes of the species *P. resedaeformis*, 100x magnification. All scale bars indicate 100 µm.

Pre-vitellogenic: Small oocytes, consisting of a thin mesogleal envelope, lacking development of a thick cortical granular layer. Observed closely to mesenteric lamellae. Transition from previtellogenic to vitellogenic oocytes takes place at ~ 233.33 µm in *P. resedaeformis* and at ~ 100 µm in *P. placomus*.

Vitellogenic: Larger oocytes, consisting of a granular yolk and development of a thick cortical granular layer enveloping the cell. Observed centrally towards the aboral end of the gastrovascular cavity and in one instance within the longitudinal compartment/tentacle cavity.

For male individuals, spermatocysts were staged (Waller *et al* 2002; Waller and Tyler 2005; Mercier and Hamel 2011) and provided insight into reproductive timing based on developmental progression (**Figure 4**).

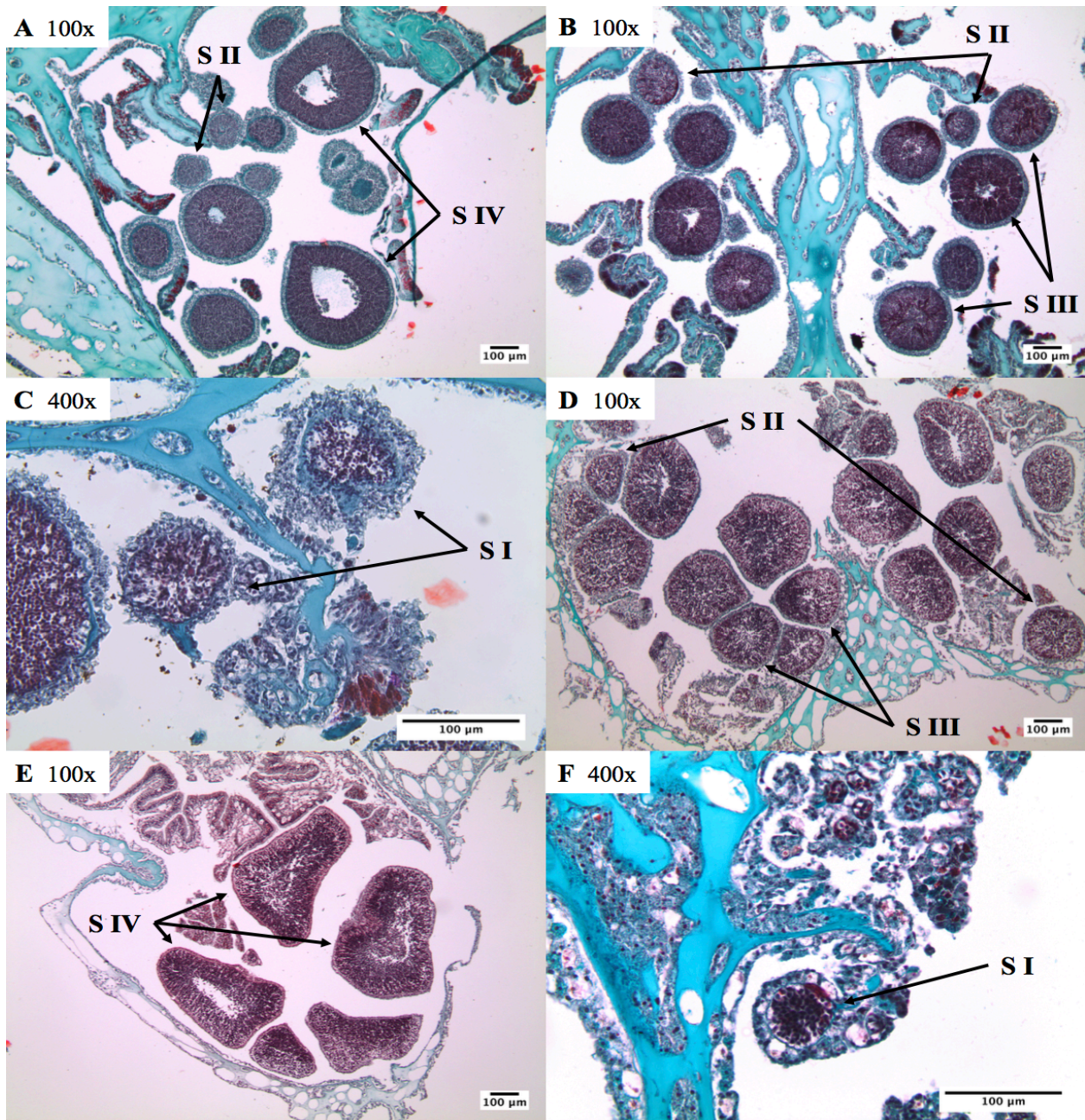


Figure 4. The stages of spermatogenesis in *P. resedaeformis* and *P. placomus*: **A-C** show identifiable stages within the species *P. resedaeformis*; **D-F** show identifiable stages within the species *P. placomus*. **S I** stage one, **S II** stage two, **S III** stage three, and **S IV** stage four. Note magnifications included within photographs, all scale bars indicate 100 µm.

Stage I: Small spermatocysts enveloped by a thin mesogleal membrane often seen with attached pedicel/peduncle.

Stage II: Larger spermatocyst, absence of pedicel/peduncle, containing loosely packed and uniformly distributed spermatids.

Stage III: Increased density and “organization” of spermatids which are at this point starting to develop into spermatozoa. Lumen becoming distinct towards the center of the spermatocyst.

Stage IV: Substantial spermatocysts with increasingly large lumen, developing spermatozoa packing and lining the mesogleal envelope.

Spermatogenesis

Male colonies exhibited variable developmental trends based on location (**Figure 5**). Individuals from the Outer Schoodic Ridge (OSR), Nygren-Heezen InterCanyon (NHI), Corsair Canyon (CC), and George’s Canyon (GC) consisted of larger proportions of stage IV spermatocysts than Western Jordan Basin (WJB) and Central Jordan Basin (CJB). Data were analyzed categorically using contingency tables and then calculating a Pearson’s χ^2 test to discern whether differences in spermatocyst stages were statistically different between sampling locations. Both species showed statistical difference ($p < 0.05$) based on sampling locations. A Bonferroni pairwise comparisons *post hoc* test was run to control familywise error rates. In each comparison, there were statistically

significant differences between locations except between *P. placomus* samples from the 2014 WJB and CJB locations as well as *P. resedaeformis* colonies from Corsair and George’s Canyon.

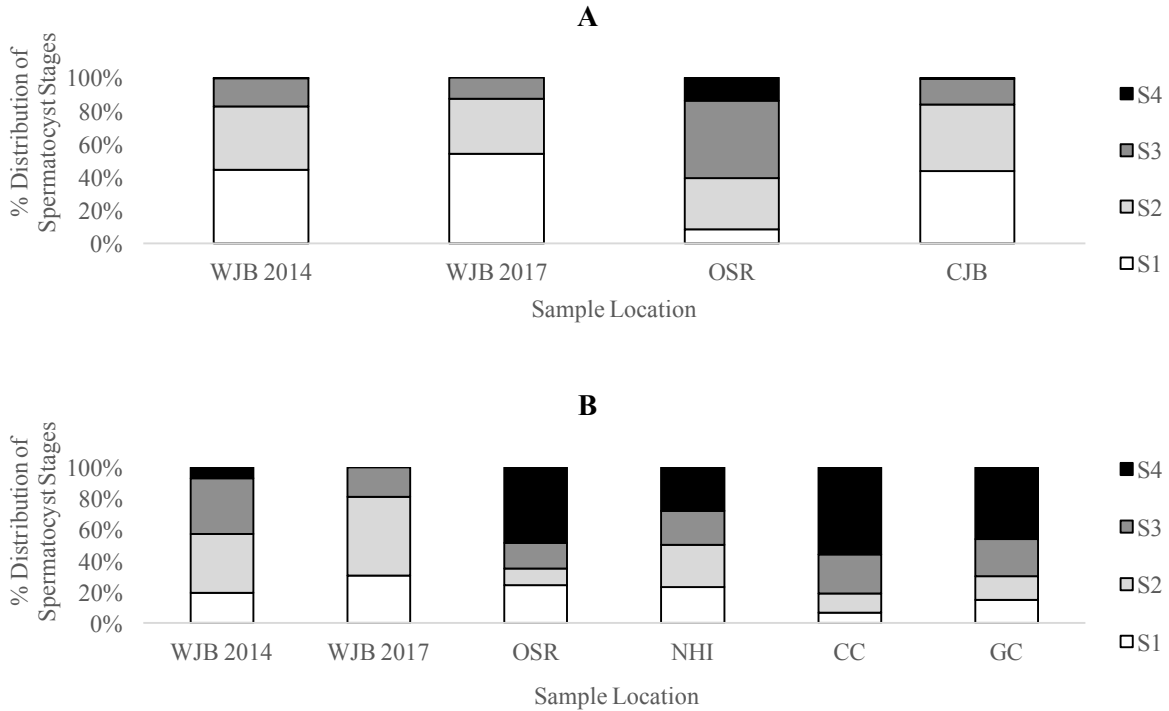


Figure 5. Developmental distribution of spermatocysts based staging scheme (Figure 4). **A** *P. placomus* separated by location, N = 25 male samples analyzed. **B** *P. resedaeformis* separated by location, N = 27 male samples analyzed.

Oocyte Diameter and Height Distribution

Females examined also exhibited differences in oocyte size, as well as colony heights, between *P. placomus* and *P. resedaeformis* (Figure 6). The mean oocyte diameter among *P. placomus* samples was 64µm and the mean colony height was 11cm. *P. resedaeformis* colonies and oocyte diameters were roughly 2.3 x larger on average consisting of a mean oocyte diameter of 140µm and a mean colony height of 26cm. Interestingly, even though *P. resedaeformis* colonies and oocytes are ~ 2.3 x larger on average, than *P. placomus*, the average oocyte size is 0.0006 x the colony height for both species. This provides evidence to support the hypothesis that oocyte size

scales proportionally with species size. In each histogram (**Figure 6**) the distributions are heavily skewed to the right, showing the predominance of smaller oocytes and coral colonies. Descriptive statistics are provided in **Table 2** summarizing the major trends of these data. The median was used, as a more representative measure of center, due to heavily skewed distributions, while statistically analyzing differences between subpopulations and seasonal variability. In the following sections, “Differences Among Subpopulations” and “Seasonal Reproductive Variability”, these trends, seen in **Figure 6**, are further dissected to investigate the underlying differences in reproductive variability based on sampling locations.

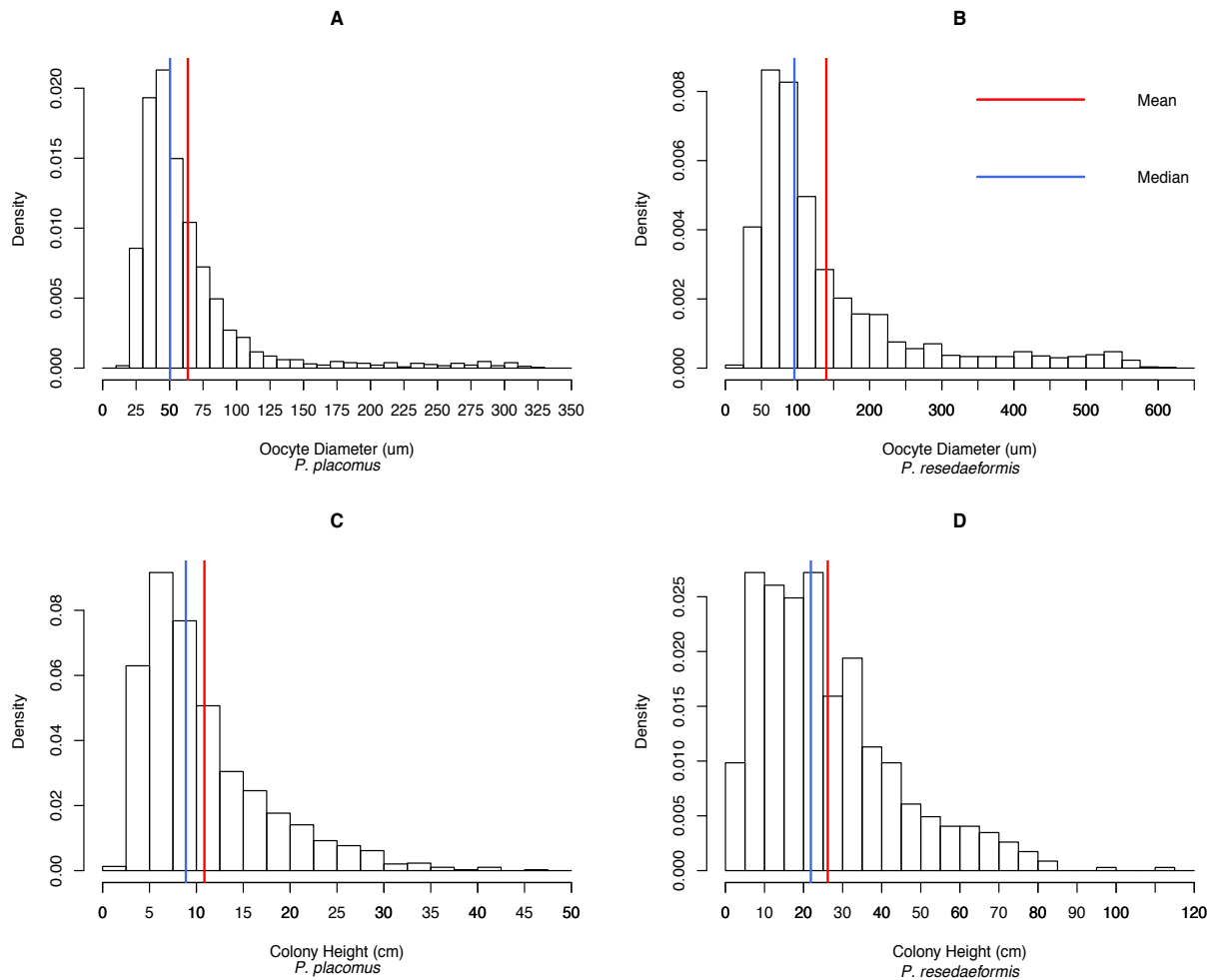


Figure 6. Histograms showing the frequency distribution of oocyte feret diameters and colony heights, between *P. placomus* (left) and *P. resedaeformis* (right). **A** *P. Placomus*, N = 21 female colonies sampled from and n = 2324 oocyte diameters measured. **B** *P. resedaeformis*, N = 23 female colonies sampled from and n = 2274 oocyte diameters measured. **C** *P. placomus*, n = 1563 colony heights measured. **D** *P. resedaeformis*, n = 691 colony heights measured.

Table 2. Descriptive statistics summarizing the data in **Figure 6**.

Species	Oocyte Diameter (μm)			Colony Height (cm)		
	Mean	Median	Skewness	Mean	Median	Skewness
<i>P. placomus</i>	63.61	50.36	3.06	10.86	8.88	1.48
<i>P. resedaeformis</i>	139.85	95.57	1.95	26.19	21.86	1.14

Differences Among Subpopulations

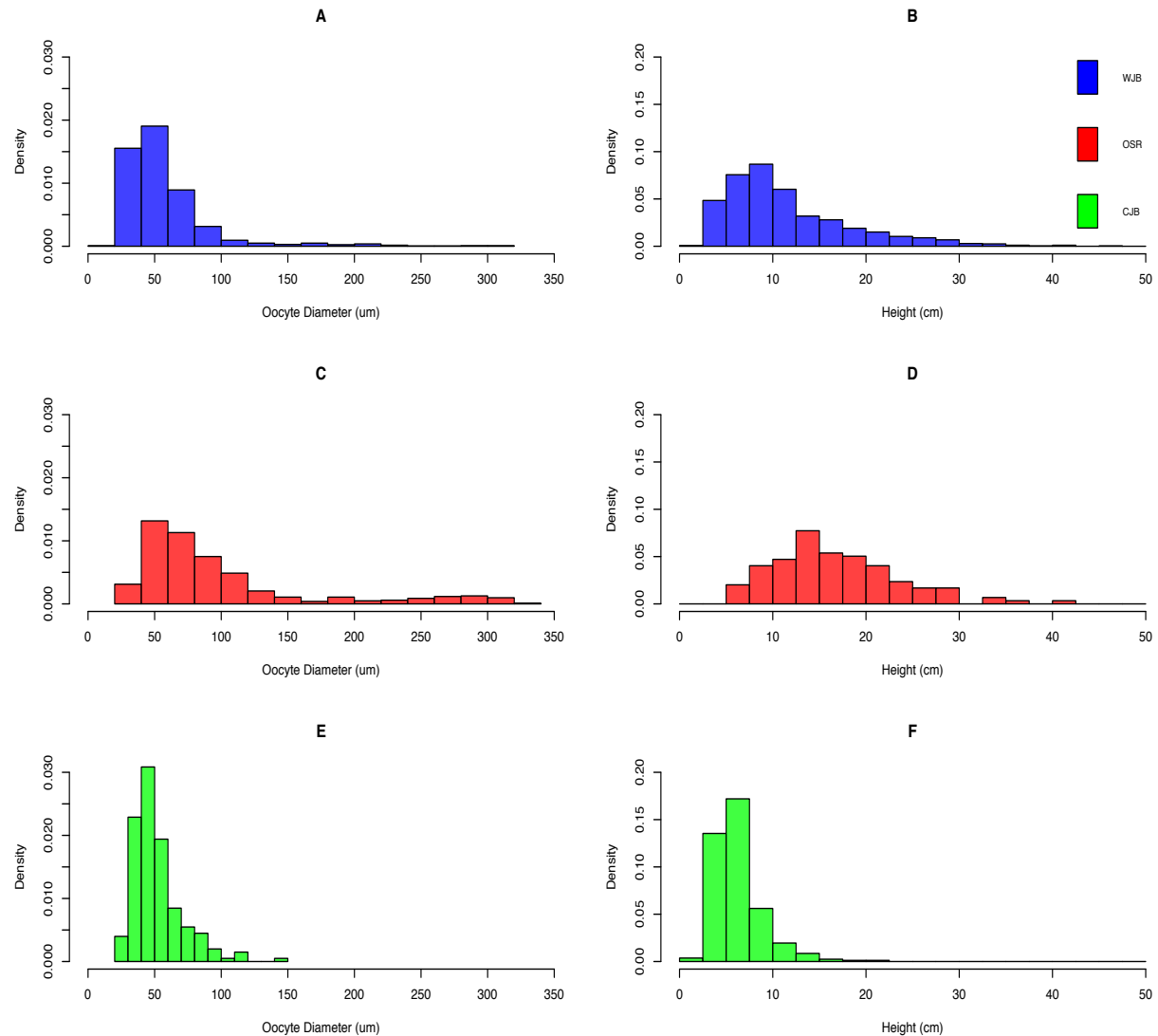


Figure 7. *P. placomus*, Histograms showing the difference in oocyte diameter (left) and colony height (right) distributions between 2014 sampling locations. Legend depicts sampling location by color. **A** $N = 10$ colonies sampled from and $n = 1210$ oocyte diameters measured. **B** $n = 1116$ colony heights measured. **C** $N = 4$ colonies sampled from and $n = 513$ oocyte diameters measured. **D** $n = 119$ colony heights measured. **E** $N = 3$ colonies sampled from and $n = 201$ oocyte diameters measured. **F** $n = 328$ colony heights measured.

Differences in oocyte size and height distributions between sampling locations of *P. placomus* colonies (**Figure 7**), show a snapshot of oogenesis, as well as colony height differences, suggesting reproductive variation between coral subpopulations. The Outer Schoodic Ridge subpopulation shows proportionally more vitellogenic to previtellogenic oocytes (based on oocyte size), in addition to larger colony sizes, than other sample locations.

When analyzing both oocyte diameter and height distributions, q-q plots (quantile quantile) were visually examined showing strong right skewness, much like total distributions. In addition, Shapiro-Wilk normality tests were run and provided significant results ($p < 0.05$), thus supporting that these data do not follow a normal distribution. As a result, in both instances, a Kruskal-Wallis non-parametric analysis of variance was run as it does not assume a Gaussian (normal) distribution. Test results indicate that both data streams, oocyte size and height distributions, show statistical significance between locations ($p < 0.05$) and a Dunn *post hoc* test was performed to further analyze pairwise comparisons between each subpopulation. The Dunn *post hoc* test was run using a Benjamini-Hochberg p -value adjustment method, advantageous for decreasing false discovery rates. Test results showed a statistically significant difference between oocyte diameters among the Outer Schoodic Ridge and Western/Central Jordan Basin subpopulations of *P. placomus* ($p < 0.05$). This same test showed a non-statistical difference in oocyte size between Western Jordan Basin and Central Jordan Basin ($p > 0.05$). A Dunn *post hoc* test was also run looking at pairwise comparisons between colony heights which showed statistical significance among each subpopulation ($p < 0.05$). In summation, these results further suggest that at the point in time when these data were collected, there was a significant difference in reproductive timing and oocyte size between subpopulations of *P. placomus*.

Like *P. placomus*, *P. resedaeformis* also showed variation in oocyte size and colony height among sampling locations. Data were analyzed following the same statistical framework as *P. placomus* by first exploring homogeneity and homoscedasticity, contingent upon which further analysis was performed. Similarly, both the oocyte diameter and height distribution of *P. resedaeformis* (**Figure 8**), violated the assumption of normality when visually analyzing q-q plots and further evaluation using a Shapiro-Wilk normality test. Distributions showed right skewness and were further analyzed using a Kruskal-Wallis non-parametric analysis of variance. Kruskal-Wallis tests showed statistical significance ($p < 0.05$) interpreted as a difference in both oocyte size and colony size between *P. resedaeformis* subpopulations.

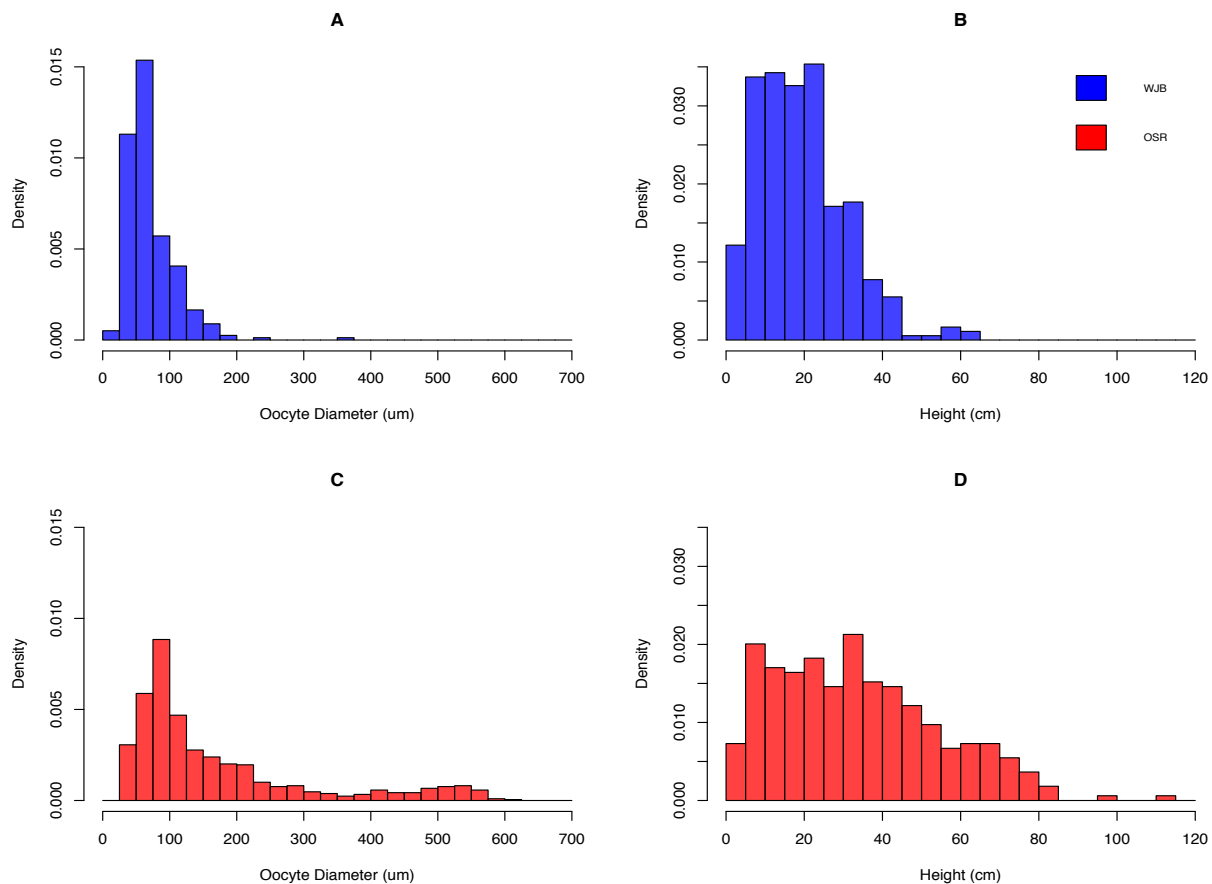


Figure 8. Histograms showing the difference in *P. resedaeformis* oocyte diameter (left) and colony height (right) distributions between 2014 sampling locations. **A** N = 5 colonies sampled from and n = 315 oocyte diameters measured. **B** n = 362 colony heights measured. **C** N = 6 colonies sampled from and n = 837 oocyte diameters measured. **D** n = 329 colony heights measured.

Pairwise comparisons, provided by a Dunn *post hoc* test using a Benjamini-Hochberg p -value adjustment showed a statistically significant difference in oocyte size between all subpopulations ($p < 0.05$), except for between Outer Schoodic Ridge and 2017 Western Jordan Basin 2014 ($p > 0.05$).

Seasonal Reproductive Variability

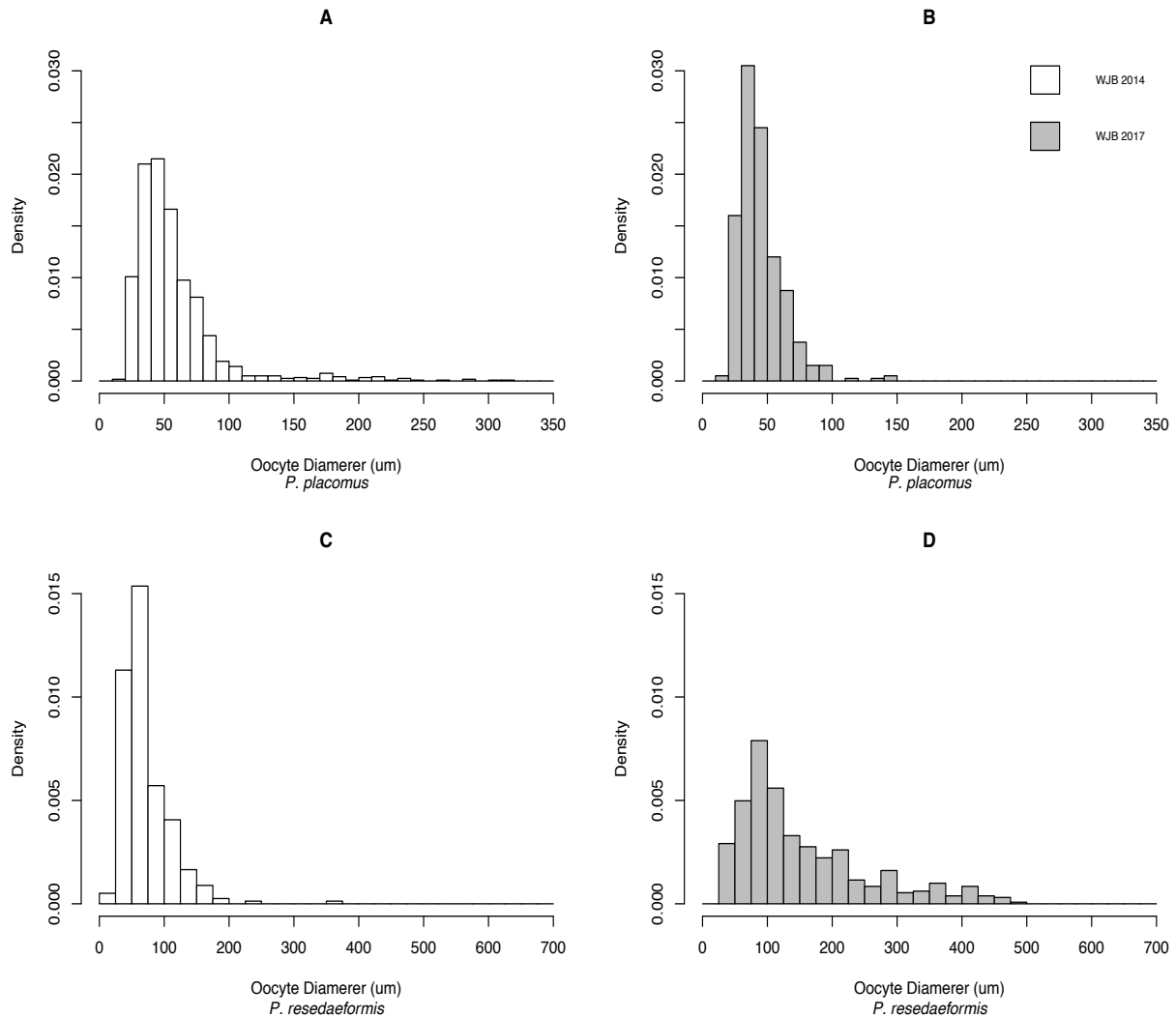


Figure 9. Comparison of oocyte diameters between August 2014 and June 2017 among both *P. placomus* (Top) and *P. resedaiformis* (Bottom). **A** N = 10 colonies sampled from and n = 1210 oocyte diameters measured. **B** N = 4 colonies sampled from and n = 400 oocyte diameters measured. **C** N = 5 colonies sampled from and 315 oocyte diameters measured. **D** N = 6 colonies sampled from and 522 oocyte diameters measured.

Repeat sampling from the Western Jordan Basin (WJB) from August 2014 and June 2017 allowed for seasonal variability of reproductive development to be investigated for both *P. placomus* and *P. resedaeformis* (**Figure 9**). This difference, supported statistically by a Mann-Whitney U test ($p < 0.05$) provided evidence to support that there exists not only spatial variation of reproductive development but seasonal variation as well among coral species and subpopulations within the Gulf of Maine.

Fecundity

In addition to looking at the distributions of oocyte sizes between locations species variation in fecundity was analyzed (**Figure 10**). Fecundity data, measured by the number of oocytes per polyp, also showed variation between sampling locations, and even potential seasonal variability when looking at samples from Western Jordan Basin 2014 and Western Jordan Basin 2017. Average quantities shown express mean \pm 1SE. The average fecundity per polyp, across all female samples, was 23.4 ± 4.3 oocytes per polyp for *P. placomus* and 16.5 ± 2.5 oocytes per polyp for *P. resedaeformis*. These boxplots also show substantial ranges in fecundity of *P. placomus* (0.33-86 oocytes per polyp) and *P. resedaeformis* (2-49 oocytes per polyp).

Fecundity data were analyzed by first checking assumptions of homogeneity and homoscedasticity. To do this q-q plots were visually analyzed and supported by Shapiro-Wilk normality testing. *P. placomus* fecundity data showed slight deviation from normality whereas *P. resedaeformis* fecundity data showed normality. Follow up, to affirm homoscedasticity, was done with Levene tests. Again, *P. placomus* fecundity data was slightly heteroscedastic whereas *P.*

resedaeformis remained homoscedastic. Since *P. placomus* data showed deviations from normality they were analyzed using a Kruskal-Wallis non-parametric analysis of variance. This is important to note, since when running these same data through the parametric version of this test (one-way ANOVA) a significant signal was detected, albeit marginally ($p < 0.1$), giving onus to testing data assumptions. However, as *P. placomus* data were analyzed using a Kruskal-Wallis non-parametric analysis of variance, there was no detection of significance between fecundity based on difference in subpopulation location. Passing all test assumptions, *P. resedaeformis* fecundity data were analyzed parametrically using a one-way ANOVA. This test resulted in a statistical significance ($p < 0.05$), showing that there is difference between locational fecundities of *P. resedaeformis* colonies. Further analysis, to identify which locations showed statistical differences, was performed using a Bonferroni pairwise comparisons *post hoc* test. Pairwise comparisons identified that the only two locations to show a statistical difference ($p < 0.05$) were the 2014 Western Jordan Basin and Corsair Canyon subpopulations.

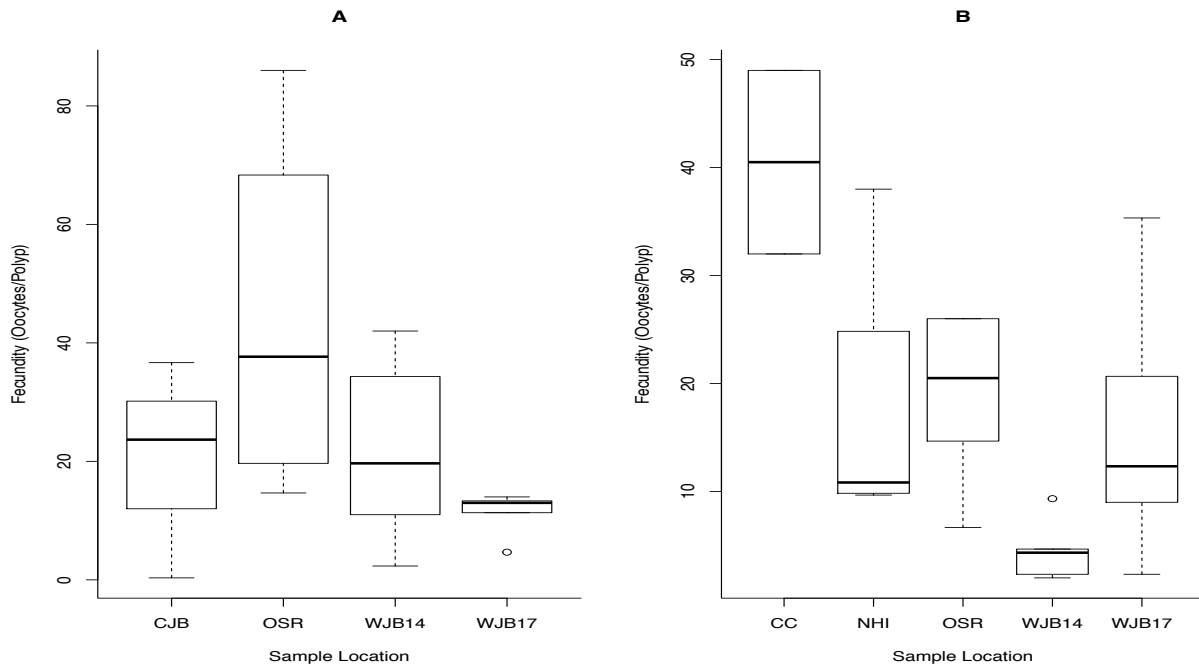


Figure 10. Boxplots of the fecundity distributions between sampling locations. **A** *P. placomus*; N = 21 female samples and **B** *P. resedaeformis*; N = 23 female samples.

Morphometric Regression Analyses

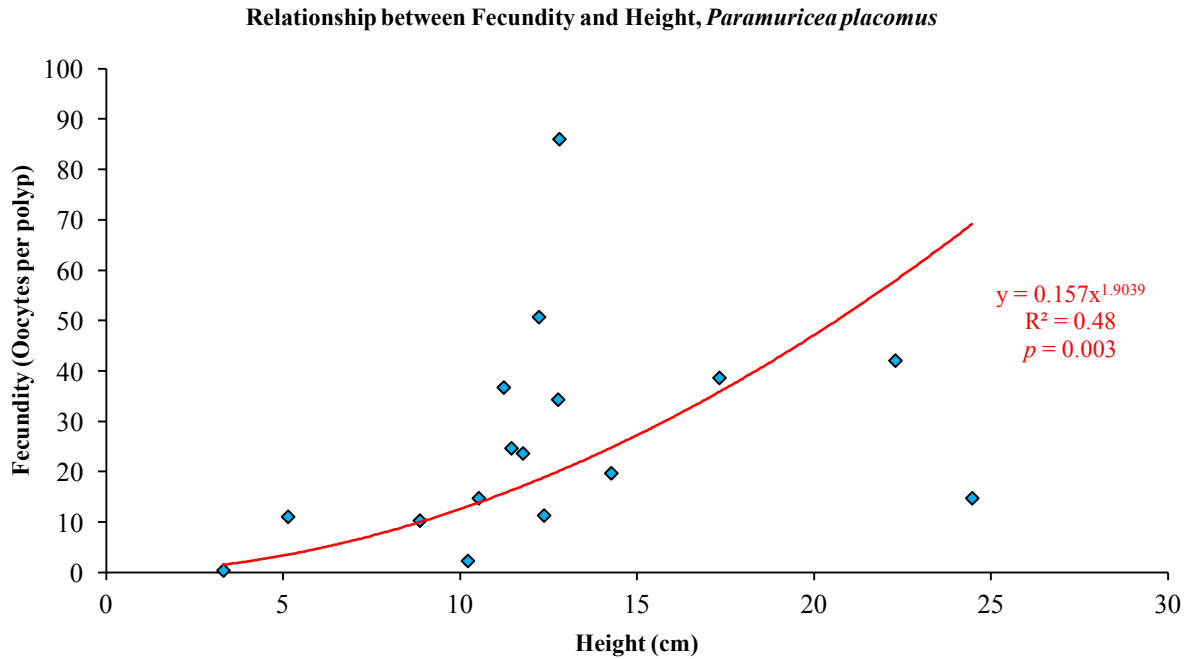


Figure 11. Regression analysis providing the mathematical relationship between height and fecundity of *P. placomus*. **Equation 5.**

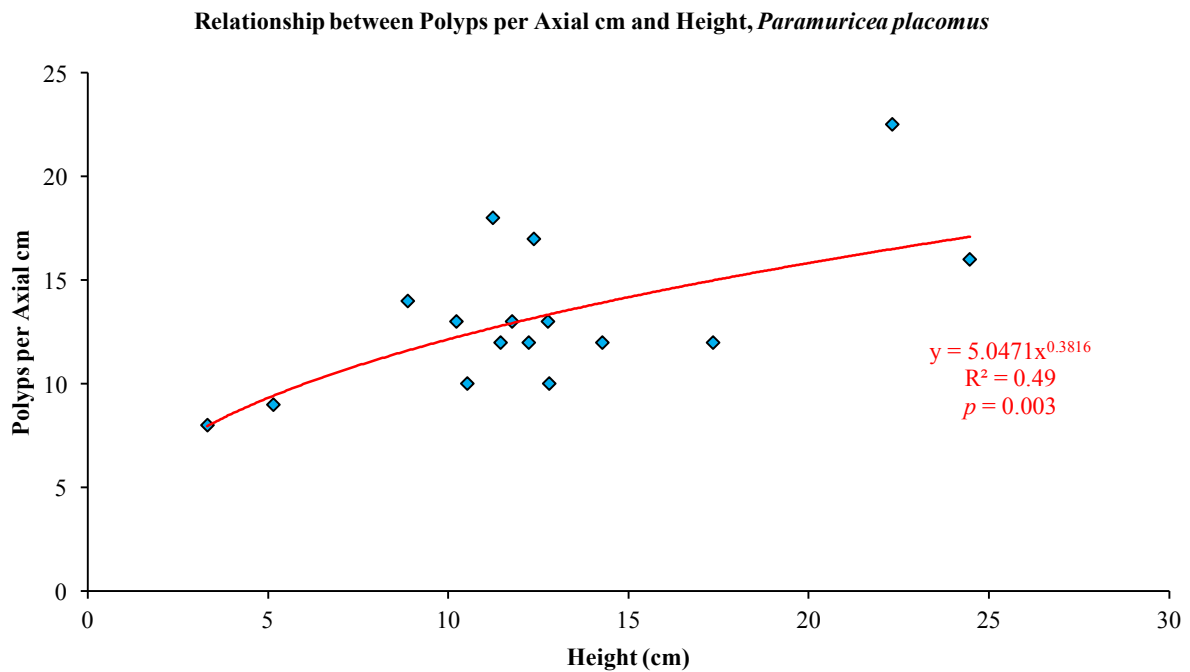


Figure 12. Regression analysis, of *P. placomus*, providing the mathematical relationship between height and polyps per axial cm. **Equation 6.**

Fecundity, polyps per axial cm, and total branch length were regressed with colony heights to develop quantifiable relationships used to inform a cohesive model for estimating the reproductive potential of entire coral colonies. To do this multiple regression models had to be run to more accurately define the functional relationships between variables (**Equation 4**) and colony height. By further defining these functional relationships, more dynamic estimations are made as they account for calculated changes between variables instead of stagnant averages.

Power function regression models were fit to these data as they provided better coefficients of determination (Fecundity: $R^2 = 0.48$, Polyps/Axial cm: $R^2 = 0.49$, and Total Branch Length: $R^2 = 0.78$), accounting for a higher proportion of variance shared by the data than simple linear models (**Figure 11, 12, and 13**). All models were tested using Akaike's Information Criterion (AIC) providing further evidence that power function regression models were the best fit. In addition, a Pearson's correlation test was run, on all three regression models, confirming statistical significance ($p < 0.05$). The relationship between total branch length (TBL) and height, R^2 value of 0.78, was strikingly similar to the coefficient of determination obtained by Mistri (1995), R^2 value of 0.77, when also assessing the relationship between TBL and height of *Paramuricea clavata*, in the Mediterranean. This may be attributable to strong morphotyping of this genus, showing a tendency towards planar growth, a strategy for utilizing nutrient uptake in uni- and bi-directional flows (Mortensen and Buhl-Mortensen 2005).

These resulting functional relationships thus allow for colony height to be used as relatively accurate proxy measurement for the changes in fecundity, polyps/axial cm, and total branch length of *P. placomus* colonies. These relationships, as expressed for *P. placomus* in **equation 5, 6, and**

7, are of importance for accurately calculating the total reproductive potential of colonies among this species.

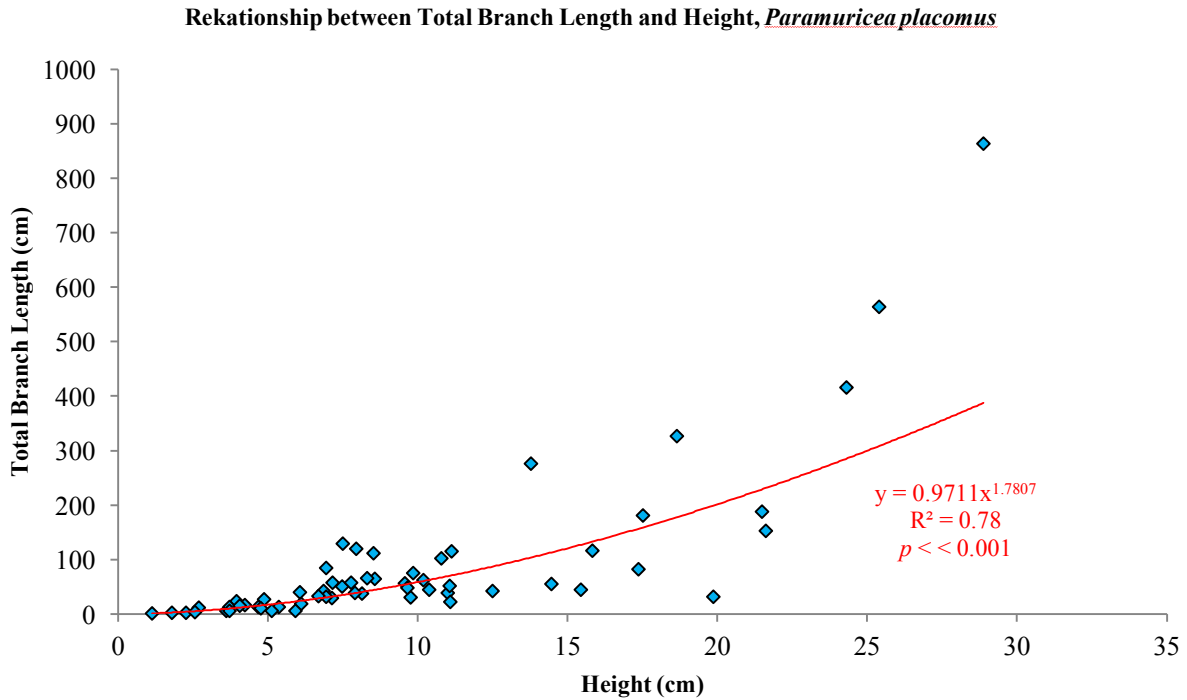


Figure 13. Using HD video analysis 59 individual colonies of *P. placomus* were analyzed and an exponential regression was used to develop a functional relationship between colony height and Total Branch Length (TBL). **Equation 7.**

Resampling, especially on the minimum and maximum ends of the colony size range, is important for increased interpolative accuracy, as it is an unlikely assumption that fecundity per polyp will continue to increase exponentially as the colony grows because of internal polyp space being an eventual limitation (Fadlallah 1983; Sebens 1987; Hall and Hughes 1996).

These same functional relationships have been difficult to quantify with *P. resedaeformis* colonies as they show less consistency in their growth and tend towards more three-dimensional arborescent morphologies, making them unquantifiable on a two-dimensional screen. As a result, to develop

a similar height to total branch length relationship, full colony collections or museum specimens may be the only option for elucidating such a relationship. However other relationships were investigated such as fecundity, polyps/axial cm, and height. Sample size was minimal, as corresponding height measurements of sampled colonies were elusive. Data were pooled between 2014 and 2017 cruises, to increase the sample size.

Linear regression models were used to analyze the relationship between fecundity and height as well as the relationship between polyps/axial cm and height, for *P. resedaeformis* samples (**Figure 14 and 15**). AIC model evaluation was run to determine which linear functions were the best fit. A logarithmic linear model was selected ($R^2 = 0.47$), to describe the relationship between fecundity and height, over a linear model, even though the linear model had a higher coefficient of determination ($R^2 = 0.52$) and lower AIC score. This decision was made as it is reasonable to infer that this relationship is more likely to reach an asymptote than continue to increase linearly indefinitely, as described previously with *P. placomus*. Additionally, the relationship between polyps/axial cm and height was analyzed using a second order polynomial function as this linear model provided the highest coefficient of determination ($R^2 = 0.30$). Again, much like *P. placomus*, biological limitations impose the improbability of ever increasing mathematical functions when evaluating how polyps/axial cm and height are related. A best fit second order polynomial function suggests that polyps/axial cm increase initially then decrease as the colony continues to grow. This may be the result of colonial compensation for decreasing particle capture rates as colony sizes increase (McFadden 1986), thus having fewer polyps and reducing intracolony competition and the cost of excess vegetative growth. Both relationships were further evaluated using a Pearson's correlation resulting in statistical significance ($p < 0.05$).

Functional relationships, established by quantifying reproductive development and colony morphologies, are an important component required to formulate a comprehensive model, used to estimate both potential relative fecundity (PRF) and effective relative fecundity (ERF) for entire coral colonies (*in sensu* Mercier and Hamel, 2011).

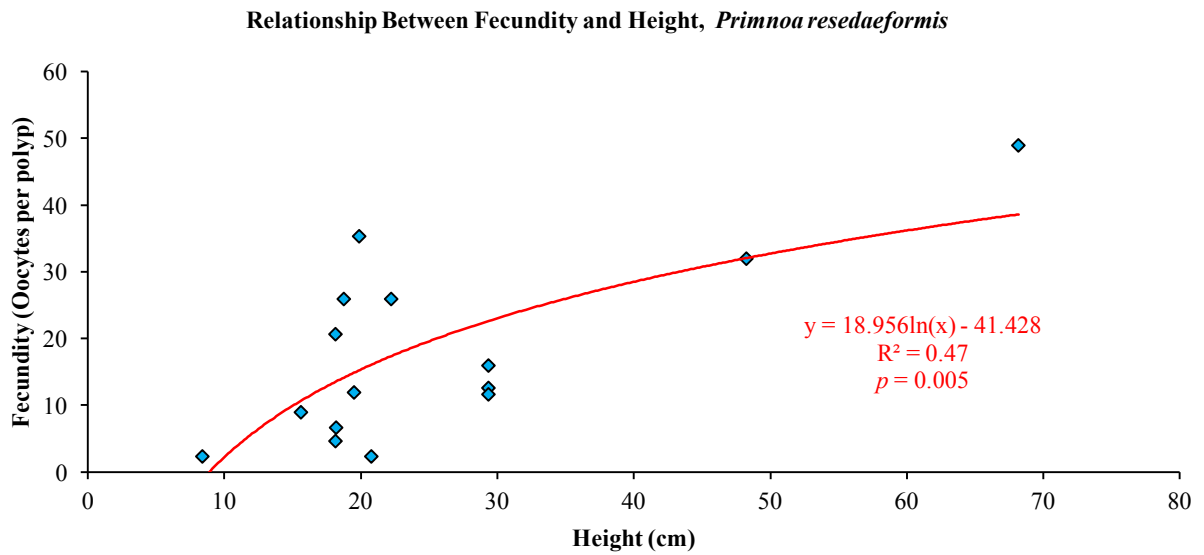


Figure 14. Regression analysis providing the mathematical relationship between height and fecundity of *P. resedaeformis*. **Equation 10.**

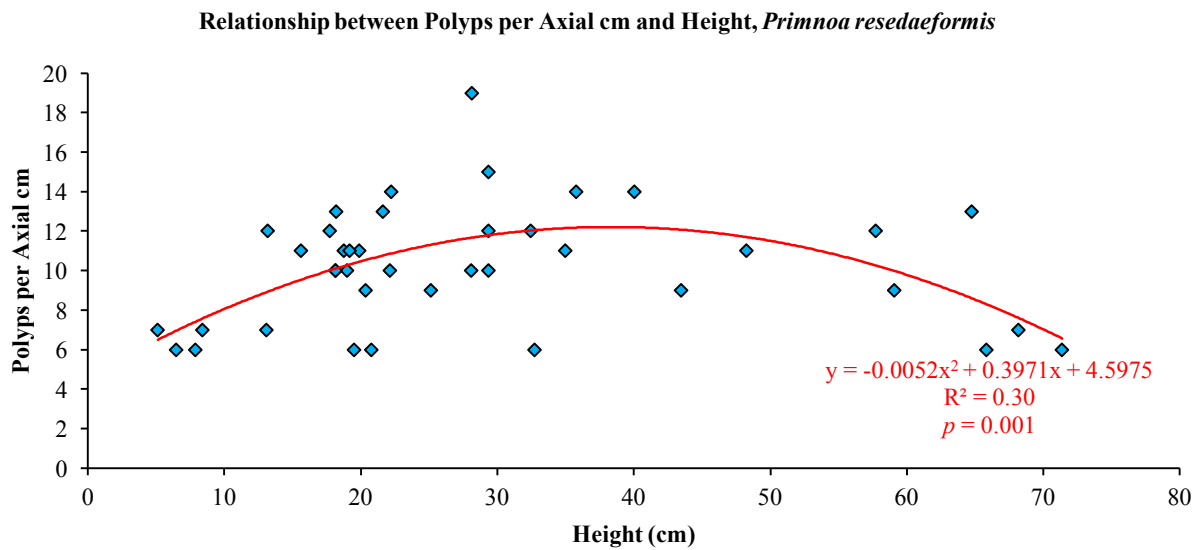


Figure 15. Regression analysis, of *P. resedaeformis*, providing the mathematical relationship between height and polyps per axial cm. **Equation 11.**

Size and Age at Maturation

Maturation, evaluated as a gradient, rather than stark division established by average colony size, may be a more informative approach when considering dynamic biological organisms. To account for this, standard errors (± 2 SE) have been included to establish colony size ranges encompassing the stage of reproduction/non-reproduction being discussed. State of maturation was identified based on presence (mature) and absence (immature) of vitellogenic oocytes for females and spermatocyst staging (Stage I and II, immature / Stage III and IV mature) for males. It is important to note that male gametogenesis is often more difficult to gauge (Tyler *et al* 1982), however maturation at Stage III is also suggested by Mercier and Hamel (2011), resultant of spermatozoa prominence within spermatocysts. The following estimations of colony age at corresponding height are derived from an average annual growth of 0.56 cm/year (Sherwood and Edinger 2009), assuming a constant and continuous growth rate for *P. placomus* (**Table 3**).

Table 3. *P. placomus*: Range in reproductive maturation expressed as size and time.

<i>P. placomus</i>	Average Height (cm)	Age (years)	SE Size Range (cm)	Age Range (years)
Non-Reproductive	8.8	15.7	4.7 – 12.9	8.4 – 23.0
Female				
Immature	9.4	16.8	6.4 – 12.4	11.4 – 22.1
Mature	15	26.8	11.6 – 18.5	20.7 – 33.0
Male				
Immature	9.9	17.7	6.3 – 13.5	11.25 – 24.1
Mature	17.6	31.4	14.5 – 20.7	25.9 – 37.0

These same data were collected for *P. resedaeformis* colonies (**Table 4**), however, work done by Mortensen and Buhl-Mortensen (2005) provide a functional relationship between height and age

showing changes in growth rate over time (**Equation 2**). This modeled relationship provides more informative estimations of age as it does not assume a constant and continuous growth rate. When solved for age, this equation (**Equation 3**) can also be used to calculate the age of *P. resedaeformis* colonies based on their height. Importantly, **equation 2** was derived from data collected from the Northeast Channel, south of Nova Scotia, which is in close geographical proximity to the data collected in this study.

Equation 2.
$$Height = 27.194 \ln(Age) - 36.859$$

Equation 3.
$$Age = e^{\frac{Height+36.859}{27.194}}$$

Table 4. *P. resedaeformis*: Range in reproductive maturation expressed as size and time.

<i>P. resedaeformis</i>	Average Height (cm)	Age (years)	SE Size Range (cm)	Age Range (years)
Non-Reproductive	9.2	5.4	1.1 – 17.2	4.0 – 7.3
Female				
Immature	19.0	7.8	12.3 – 25.7	6.1 – 10.0
Mature	29.0	11.3	18.3 – 39.5	7.6 – 16.6
Male				
Immature	11.3	5.9	6.1 – 16.4	4.9 – 7.1
Mature	36.5	14.8	28.7 – 44.3	11.1 – 19.8

Size at maturation estimates, growth rates, and morphometric data, provide the relationships necessary to begin estimating entire colony PRFs and ERFs while progressing towards calculated annual changes in reproductive effort. In the following section this will be investigated in further detail by explaining the intersection of these data streams and providing a mathematical model for calculating the reproductive effort of entire coral colonies.

Modeling Reproductive Potential

“All models are wrong, but some are useful”

-George Box

Mathematical modeling was used to estimate the potential relative colony fecundity (F) and effective relative colony fecundity (Fv), and is the culmination of data collected throughout this and prior investigations. Each variable was selected based on the logical progression building from individual gamete to entire colony (**Equation 4**). The idea that the polyp, as a single modular unit, forms a larger colony, based on asexual redundancies, is the foundation connecting coral reproductive biology to their morphology. This is not the first time the idea of modularity has been explored, as reviewed by Boardman *et al* (1973), again by Jackson *et al* (1985) and more recently in Hall and Hughes (1996). These models have been created as a means of quantifying the potential relative fecundity of entire colonies, in this case specific to *P. placomus* and *P. resedaeformis*, with the ability of using height as a proxy. A proxy measurement, such as colony height, allows for larger ecosystem scale data to be collected more efficiently and the methodology and framework, from which this model is based, can be applied laterally to other coral/colonial species.

Equation 4.
$$F = P * r(R) * T$$

Where

F , Potential relative colony fecundity

P , represents fecundity per polyp

r , is the proportion of reproductive to non-reproductive polyps per axial cm

R , polyps per axial cm

T , total branch length

Paramuricea placomus

Equation 5. $P = [0.157(H)^{1.9039}]$

Equation 6. $R = [5.0471(H)^{0.3816}]$

Equation 7. $T = [0.9711(H)^{1.7807}]$

Where

H , is the height of the coral colony

Thus

Equation 8. $F = [0.157(H)^{1.9039}] * r[5.0471(H)^{0.3816}] * [0.9711(H)^{1.7807}]$

Such that

Equation 9. $Fv = Pv \left[[0.157(H)^{1.9039}] * r[5.0471(H)^{0.3816}] * [0.9711(H)^{1.7807}] \right]$

Where

Pv , is the scaling proportion of vitellogenic oocytes

Fv , Effective relative colony fecundity

Primnoa resedaeformis

Equation 10. $P = [18.956 * \ln(H) - 41.428]$

Equation 11. $R = [-0.0052(H)^2 + 0.3971(H) + 4.5975]$

Equation 12. $T = ?$

Thus

Equation 13.

$$F = [18.956 * \ln(27.194 * \ln(Age) - 36.859) - 41.428] * T([27.194 * \ln(Age) - 36.859]) * r[-.0052(27.194 * \ln(Age) - 36.859)^2 + 0.397(27.194 * \ln(Age) - 36.859) + 4.598]$$

Such that

Equation 14.

$$Fv = Pv[18.956 * \ln(27.194 * \ln(Age) - 36.859) - 41.428] * T([27.194 * \ln(Age) - 36.859]) * r[-.0052(27.194 * \ln(Age) - 36.859)^2 + 0.397(27.194 * \ln(Age) - 36.859) + 4.598]$$

Equations 5-7 illustrate the relationship between colony height and their corresponding variables, as explained through regression analysis. These equations are then substituted back into **equation 4** and result in **equation 8**, a more complex representation, which accounts for the changes in

reproductive parameters as height varies. At the same time this allows for a single measurement to be used, height, as a predictor of potential relative colony fecundity. Now, the proportion of vitellogenic oocytes among sampled colonies of *P. placomus*, can be used as a scalar to estimate the effective relative colony fecundity (**Equation 9**). **Figure 16** shows these two equations (**8 and 9**) plotted across the size range of *P. placomus* colonies observed from video analysis. Further representation (**Figure 17**) depicts the height distributions across subpopulation locations as plotted on top of the reproductive model. This allows for quantifiable differentiation between PRF and ERF, across subpopulations, as seen in **table 5-6**. This provides a means of accessing reproductive competency based on size dependent reproductive output.

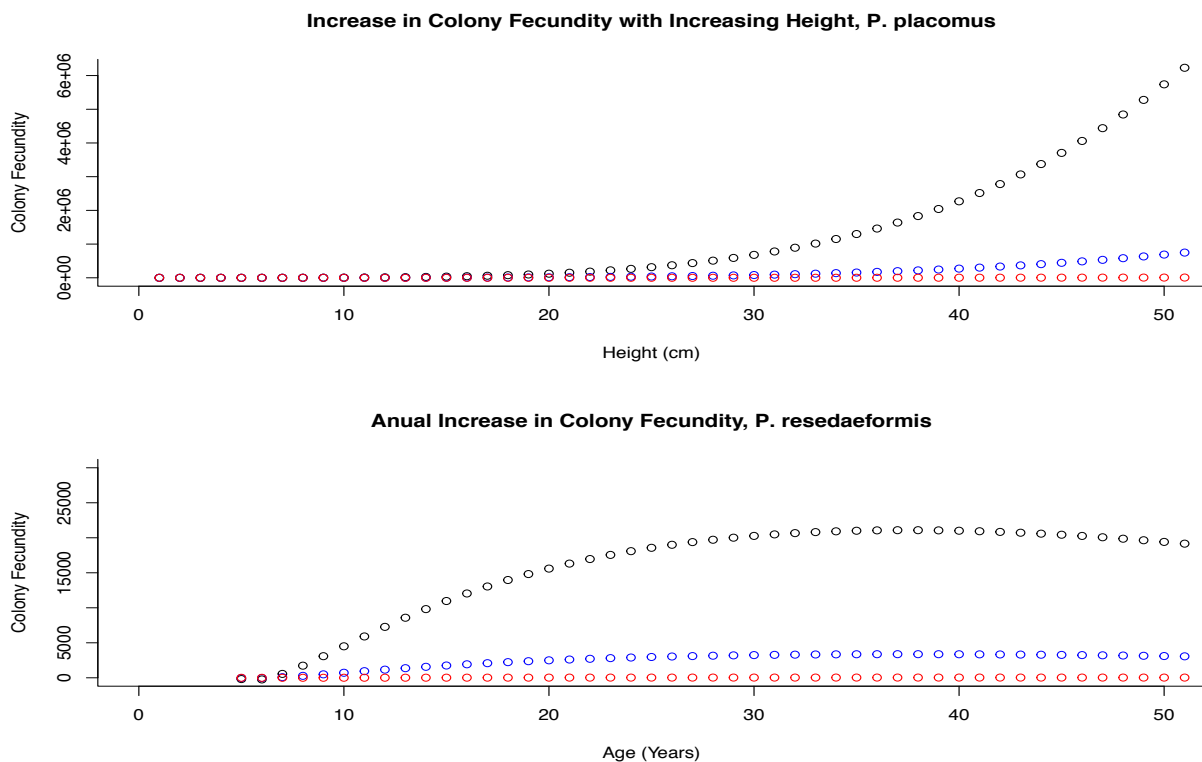


Figure 16. Modeled relationships between colony fecundity and height/age. **Top:** Plotted in black is **equation 8**, fitted with height values, 1-50 cm, spanning the range of observed *P. placomus* colonies and showing the resultant potential colony fecundity. In blue these same height values are plotted using **equation 9**, which shows the proportion of vitellogenic oocytes to potential colony fecundity. **Bottom:** Plotted in black is **equation 13**, fitted with age values, 1-50 years, spanning the range of observed *P. resedaeformis* colony ages analyzed in prior regression models. In blue these same age values are plotted using **equation 14**, showing the proportion of vitellogenic oocytes to potential colony fecundity. In red is a hypothetical 99.9% mortality curve used for graphic emphasis depicting hypothetical reproductive success.

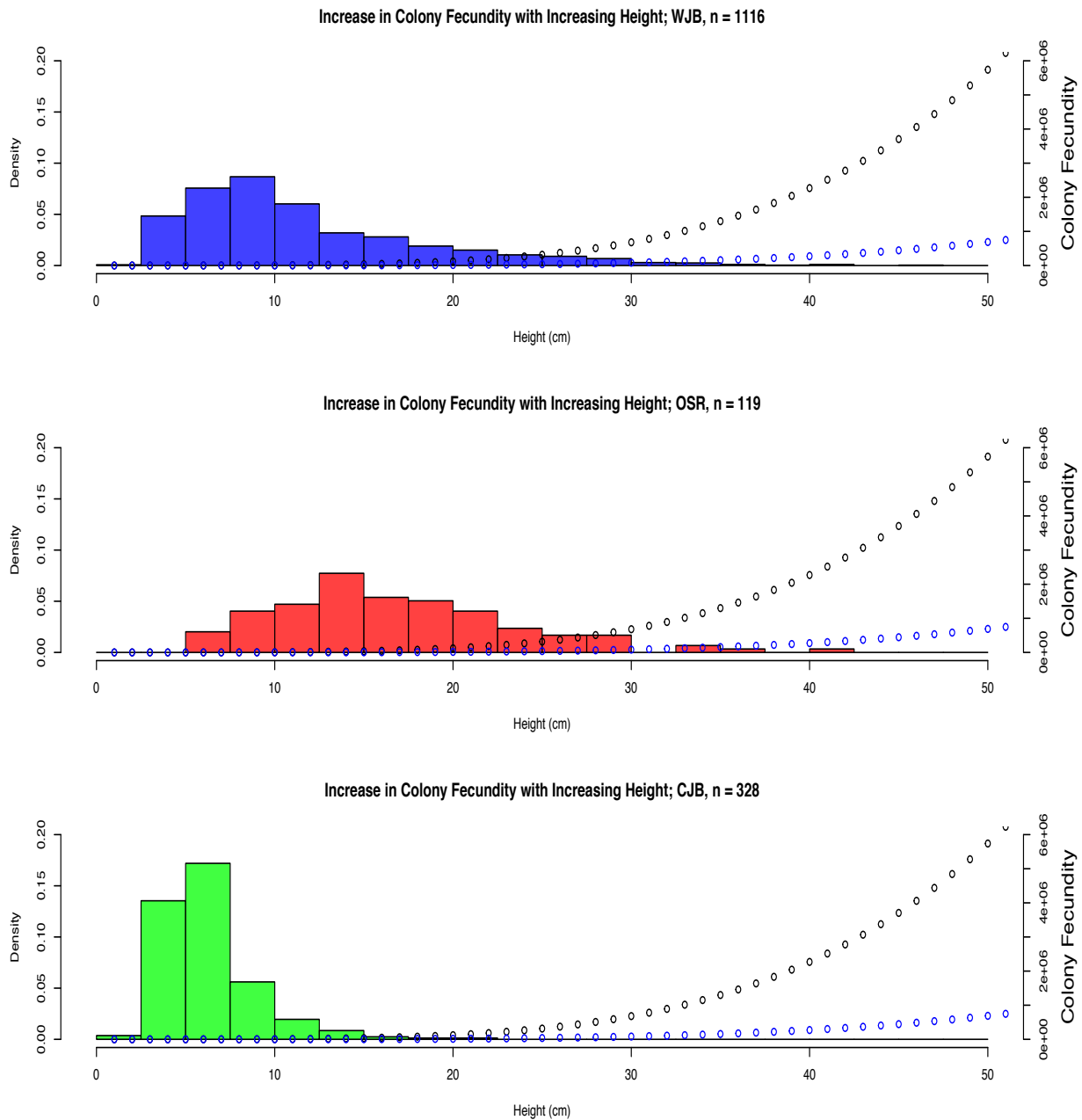


Figure 17. Height distribution frequencies, of *P. placomus*, by sampling location, plotted on top of the total fecundity (black) and proportion vitellogenic oocytes (blue) models.

Table 5. *P. placomus*: Estimated total potential fecundity, proportion vitellogenic oocytes, and age based on mean heights from sample locations. *Colonies of *P. placomus* below 8.9 cm height did not possess vitellogenic oocytes

Sample Location	Mean Height (cm)	Total Potential Fecundity	Proportion Vitellogenic Oocytes	Age (Years)
WJB	11.57	16,216	1,946	20.66
OSR	16.93	76,238	9,149	30.23
CJB	6.25	1,326	159*	11.16

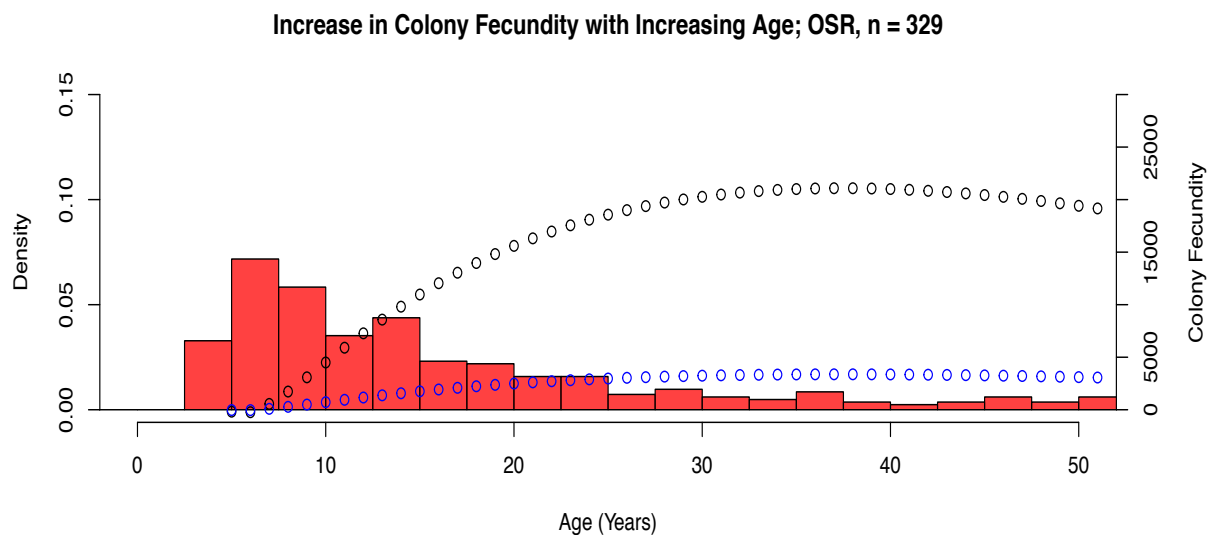
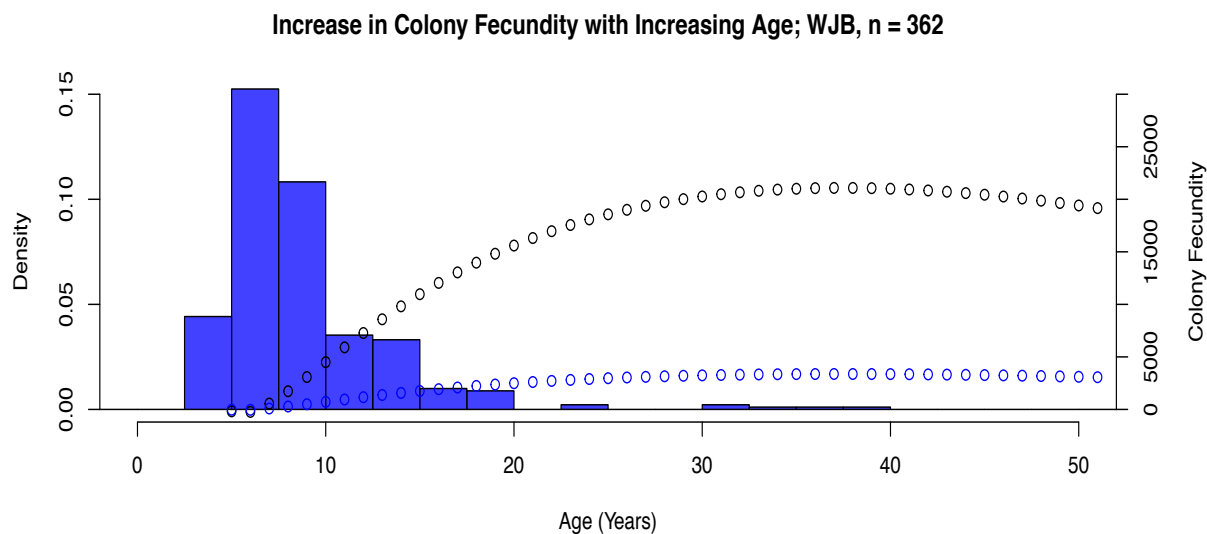


Figure 18. Calculated age distribution frequencies, of *P. resedaeformis*, by sampling location, plotted on top of the total fecundity (black) and proportion vitellogenic oocytes (blue) models.

Table 6. *P. resedaeformis*: Estimated total colony fecundities and proportion vitellogenic oocytes, and age based on mean heights from each sample location.

Sample Location	Mean Height (cm)	Total Potential Fecundity	Proportion Vitellogenic Oocytes	Age (Years)
WJB	19.38	15,877	2,540	7.91
OSR	33.68	20,983	3,357	13.38

Morphometric data were also modeled for *P. resedaeformis* colonies (**Figure 16**). These relationships were established through regression analysis and expressed as equations (**10-12**). Noticeably, **equation 12** was highlighted in red as this relationship has remained elusive and at this point is unquantified. Equations (**10 and 11**) were then substituted into **equation 4**. The relationship between colony height and age (**equation 2**), established by Mortensen and Buhl-Mortensen (2005), was then substituted in providing further iteration and resulting in **equation 13**. This is an important component as it provides the change in colony height over time thus allowing for an estimation of annual changes in RPF and ERF. As a result, modeled increase in colony fecundity with increasing age was plotted on top of age distributions of *P. resedaeformis* colonies from both the Outer Schoodic Ridge and Western Jordan Basin (**Figure 18**).

The ratio of reproductive to non-reproductive polyps per axial cm, denoted by r , was not included in any of the calculations, or the final models, as this value has yet to be determined. However, it was left in the equation and highlighted in red because of its importance to future iterations of reproductive models and will substantially contribute to increasing the accuracy of these calculations. Growth rate for *P. resedaeformis*, from Mortensen and Buhl-Mortensen's (2005) model, looking at height and age, allow for changes in colony fecundity estimations over time to be made, but the relationship between total branch length and colony size is still missing, thus drastically diminishing the total colony fecundity estimation. In addition, the relationship between total branch length and height of *P. placomus* has been modeled, which allows for a more accurate total colony fecundity estimation to be made, but it is missing the growth model showing how colony size changes over time. Essentially these are two halves of the same model with further data needed to improve either or both.

Discussion

Both *P. placomus* and *P. resedaeforms* are gonochoristic showing a similar 0.85:1 ratio of females to males. Other species of deep-sea corals show a similar 1:1 female to male ratio, but hesitations arise when being quick to round to 1. What is pertinent in both species is a reduction in female representation, testament to the energetic imbalance between female and male sexual development (Ribes *et al* 2007). Whereas the gonochoristic ratio between male and female colonies has been identified how these individuals are distributed throughout the population remains unknown. Female and male colonies of *P. placomus* and *P. resedaeformis* exhibited variation in gametogenic development between sampling locations which may coincide with differences in local reproductive timing. As a result, investigating local scale environmental drivers may be an important next step in furthering progress towards a more holistic understanding of deep-sea coral reproductive ecology.

Additionally, *P. placomus* and *P. resedaeformis* show substantial differences in oocyte size and colony size. This is important as these size differences lend themselves to potential variations in larval distribution capabilities, as larger oocytes can extend larval competency times due to an increase in nutrient reserves (Ben-David-Zaslow and Benayahu 1998; Pechenik 1999; Cordes *et al* 2001; Hwang and Song 2007), as well as overall colony reproductive capacities. Differences in average mature colony sizes (**Table 3 and 4**) may be driven by the disparity between gametogenic duration of male and female colonies of these two species, as male colonies in other octocorallians have shown drastically shorter gametogenic cycles than their female counterparts (Ribes *et al* 2007, Waller *et al* 2014). These variations in development, may result in more energy allocated

to growth, suggesting difference in growth rates between male and female colonies. Many studies investigating coral reproduction have noted the importance of colony size and the coinciding amount of time it takes to reach maturation (Sebens 1984; Sebens 1987; Soong and Lang 1992; Hall and Hughes 1996; Bak and Meesters 1998). This is especially pronounced when studying slow growth species, as it is concerning when rates of environmental change outpace an organism's ability to adapt (Connell 1978). This idea is further investigated and applied to the species of focus, *P. placomus* and *P. resedaeformis*, as they both have slow growth rates making local populations vulnerable to acute disturbances over long periods of time.

By describing and quantifying the reproductive biology of *P. placomus* and *P. resedaeformis* these reproductive data can now be used to inform individual colony and population scale estimations of reproductive potential based on morphometrics and size distribution of colonies from multiple locations across the Gulf of Maine. These linked analyses have allowed for portions of per species individual based colony reproductive potential models to be made, and has provided insight into data gaps to be filled to improve estimations. These reproductive models, used to quantify and identify regional differences in population scale fecundity, can be used during future survey work to identify key source populations, such as the Outer Schoodic Ridge and Western Jordan Basin. Key source populations contribute larger portions of gametes to the reproductive pool thus increasing recruitment potential, an essential component to sustaining local populations (Sun *et al* 2010), and increasing dispersal capabilities and connectivity among metapopulations (Morrison *et al* 2015). Individual and population scale fecundity potential estimates between locations have allowed for the identification of regional scale reproductive variability among different coral

subpopulations. As a result, it is possible to quantify differences in reproductive effort, specific to subpopulation locations, based on colony size.

When comparing colony size and oocyte size between *P. placomus* and *P. resedaeformis* it was observed that *P. resedaeformis* was ~ 2.3 x larger on average. Reproductive and colony size variability between subpopulations also highlights the likeliness of extrinsic environmental influences driving population differentiation (Sebens 1987). Importance of repeat collection to identify seasonal peaks in reproductive effort (Waller *et al* 2014) to help establish potential correlations with environmental constrains, such as nutrient fluctuations (Sebens 1984; Tyler *et al* 1984) and current velocities (Sebens 1984), driving nutrient advection, particle capture rates (McFadden 1986), and larval dispersal, are important next steps in understanding more holistically the reproductive ecology of these corals.

Reproductive isolation, driven by differences in environmental parameters, are a primary component of ecological speciation (Schluter 2001; West-Eberhard 2005). As an example, in the Gulf of Maine, colony size of *Alcyonium siderium*, differentiate geographically and locally, based on current velocities (Sebens 1984). Environmental differences may also be driving reproductive potentials, as observed in *P. resedaeformis*, based on dissimilarities in oocyte size and fecundity from collections north of Labrador (Mercier and Hamel 2011) and the Gulf of Maine (this study). Northern Labrador and the Gulf of Maine represent two distinct biogeographic regions (Buhl-Mortensen *et al* 2015), distinguished by physical environmental characteristics and species distributions (Cairns and Chapman 2001). Maximum observed oocyte size from the Labrador subpopulation, among August 2005 and July 2006 collection, was $\sim 1000\mu\text{m}$ and average

fecundities included 84.3 ± 3.1 oocytes per polyp (<500m) and 45.5 ± 1.7 oocytes per polyp (>500m). Within Gulf of Maine subpopulations, maximum observed oocyte size was $\sim 625 \mu\text{m}$, from July 24 – August 4 of 2014 and June 12 – 17 of 2017, and the average fecundity was 13.5 ± 2.4 oocytes polp^{-1} (<500m). These are profound differences, and as a result, it is reasonable to hypothesize that the northern Labrador region may be a more optimal habitat than the Gulf of Maine, suggesting an important relationship between geographical differences in reproductive variability resultant of environmental differences among geographic regions (Waller et al 2014). Conversely, this reduction in oocyte size and fecundity could be the result of overcrowding, interspecific competition beneficial for reducing competitive overgrowth, but detrimental to nutrient capture and growth (McFadden 1986; Sebens 1987). This may also explain why *P. resedaeformis* colonies show a high degree of morphometric plasticity as this is believed to dampen the effect of intraspecific competition (Hoogenboom et al 2008), and increase adaptability to environmental heterogeneity (Stearns 1989; Shaish et al 2007; Rowley et al 2015).

P. resedaeformis, within the Gulf of Maine, exist towards the upper thermal limit observed in this species, interquartile range $4.5 - 7.5^{\circ}\text{C}$ (Buhl-Mortensen et al 2015), with temperatures recorded at 250m, within the Western Jordan Basin, between 6.5 and 9.5°C (Townsend et al 2015). These differences in temperature may act as divergent drivers of local selection. Latitudinal compensation, intra specific physiological adaptation to environmental gradients (often correlate with temperature), results in distinguishable differences in baseline metabolic rates, differences in temperature tolerances, and differences in reproductive processes such as egg development times (Levinton 1983a). These processes promoting minor taxonomic transitions are defined as microevolutionary change, and may be elucidated by following subpopulations as evolutionary

stepping stones (Levinton 1983b). This may be further exacerbated by the fact that the Gulf of Maine, one of the fastest warming bodies of water on the planet (Pershing 2015), is also experiencing seasonal changes in phenology which has the potential to interrupt the timing of food web associations (Thomas *et al* 2017). The offset of these food web associations, in addition to “seasonal lag”, hypothesized here as: regional differences in the timing and intensity of surface productivity resulting in variability in vertical nutrient fluctuations, may result in the discontent between reproductive timing among coral subpopulations. As a result, the Gulf of Maine may provide a steep environmental gradient, deterministic of the rate of species divergence, based on the biogeographic adaptability and genetic isolation of *P. resedaeformis* (Morrison unpublished data) and *Paramuricea spp.* (Thoma *et al* 2009). These differences in environmental processes in addition to biogeographic differences in oocyte size and colony fecundities, may be a step along this microevolutionary gradient of which speciation is derived (West-Eberhard 2005). Evolutionary steps which have selected for the predominance of *P. resedaeformis* and *P. placomus* within the Gulf of Maine.

Conclusion

This study provides a means and demonstration of quantifying geographic differences in individual and population scale reproductive potentials, of two deep-sea coral species local to the Gulf of Maine, based on relationships between reproduction and colony morphometrics. These models are important for developing and informing continued deep-sea survey work, as height measurements are more efficient, and account for morphological complexities, thus increasing the effectiveness, and scale of future data collection. Of the three Gulf of Maine coral subpopulations surveyed, the Outer Schoodic Ridge shows the highest capacity for reproductive potential based on the average

size of individuals of both species (**Figure 17 and 18**). Colonies of *P. placomus*, based on average size, from Outer Schoodic Ridge, showed a total potential fecundity ~ 4.7 x greater than colonies from Western Jordan Basin and the Central Jordan Basin subpopulation was essentially non-reproductive (**Table 5**). Similarly, colonies of *P. resedaeformis*, based on average size, from Outer Schoodic Ridge, showed a total potential fecundity ~ 1.3 x greater than colonies from Western Jordan Basin (**Table 6**). Although there exist reproductive dissimilarities among subpopulations it is important to consider these populations holistically. These coral subpopulations act as stepping stones of dispersal, provide connectivity, and, within the Gulf of Maine, are subjected to the compounding effects of fisheries impacts, historic and present, and the inevitability of environmental change. This synergy of multiple stressors, amplifies the vulnerability of these coral habitats on individual, population, and evolutionary timescales. To protect and or mitigate future impact, dynamic conservation strategies, focused on ecosystem based management, are required.

At the foundation of this understanding sits reproduction, quintessential to a species ability to adapt and respond to change. Nevertheless, future studies addressing the relationships between colony morphometrics and growth are essential components to further evaluating the reproductive potential of these coral species. These studies will provide a means of quantifying reproductive potential changes over time, thus increasing the ability to assess recovery rates. Additional survey work quantifying population densities, development and understanding of reproductive seasonality, and coupled environmental data, are also important components to further our understanding of abiotic drivers influencing geographic differences in reproductive ecology.

Epilogue

As biologists of the deep-sea, we exist at the interface between areas of high and low dynamism. Above highly labile surface waters, and below, plates, whose movements, only the speed of geologic time can measure. We exist at a unique interface, one difficult to conceptualize and comprised of biota even more difficult to understand. Life so far removed from our own that we don't know what to do with it. Can we eat it? Does it cure ailments? What can we do with it? If not, then why is it important? All questions whose answers are applicable to merely one species, the one asking, *Homo sapiens*. If you break down the roots to our binomial nomenclature you discover that we have categorized ourselves as “wise humans”, but if you look at the Greek translation of *Homo* our new name can be extrapolated to mean “Same Wisdom”, testament to our shared consciousness and understanding. We, the newly redefined species, have thrived off our ability to ask questions, questions which now need a new direction of focus framed to consider the intrinsic importance of nature instead of its immediate value to our biological success. With a further understanding of the former comes a more sustained answer for the latter. Acknowledgment of its importance before uncertain action is taken, now more than ever, warrants strong justification. Shift the question to: Why does this not matter? vs Why does this matter? and our answers start to change. Our mindset starts to change.

REFERENCES

- Alino, P. M. & J. C. Coll, 1989. Observations of the Synchronized Mass Spawning and Postsettlement Activity of Octocorals on the Great Barrier Reef, Australia: Biological Aspects. *Bulletin of Marine Science* 45(3) 697-707.
- Andrews, A. H., E. E. Cordes, M. M. Mahoney, K. Munk, K. H. Coale, G. M. Cailliet & J. Heifetz, 2002. Age, growth and radiometric age validation of a deep-sea, habitat-forming gorgonian (*Primnoa resedaeformis*) from the Gulf of Alaska. *Hydrobiologia* 471: 101-110.
- Auster, P. J., 2005. Are deep-water corals important habitats for fishes? Freiwald A, Roberts JM (eds), 2005, *Cold-water Corals and Ecosystems*. Springer-Verlag Berlin Heidelberg, pp 747-760.
- Auster, P. J., M. Kilgour, D. Packer, R. Waller, S. Auscavitch & L. Watling, 2013. Octocoral gardens in the Gulf of Maine (NW Atlantic). *Biodiversity* 14:4 193-194. DOI: 10.1080/14888386.2013.850446
- Auster, P. J., D. Packer, R. Waller, S. Auscavitch, M. J. Kilgour, L. Watling, M. S. Nizinski, I. Babb, D. Johnson, J. Pessutti, A. Drohan & B. Kinlan, 2014. Imaging surveys of select areas in the northern Gulf of Maine for deep-sea corals and sponges during 2013-2014. Rep New England Fishery Management Council – 1 December 2014. ResearchGate DOI: 10.13140/RG.2.1.4760.0163
- Bak, R. P. & E. H. Meesters, 1998. Coral population structure: the hidden information of colony size-frequency distributions. *Marine Ecology Progress Series* 162: 301-306.
- Ben-David-Zaslow, R. & Y. Benayahu, 1998. Competence and longevity in planulae of several species of soft corals. *Mar Ecol Prog Ser* 163: 235-243.
- Bryan, T. L. & A. Metaxas, 2007. Predicting suitable habitat for deep-water gorgonian corals on the Atlantic and Pacific Continental Margins of North America. *Mar Ecol Prog Ser* 330: 113-126
- Boardman, R. S., A. H. Cheetham & W. A. Oliver, 1973. *Animal Colonies*. DH&R, Stroudsburg, PA
- Buhl-Mortensen, L. S. H. Olafsdottir, P. Buhl-Mortensen, J. M. Burgos & S. A. Ragnarsson, 2015. Distribution of nine cold-water coral species (Scleractinia and Gorgonacea) in the cold temperate North Atlantic: effects of bathymetry and hydrography. *Hydrobiologia* 759: 39-61.
- Bullimore, R. D., N. L. Foster & K. L. Howell, 2013. Coral-characterized benthic assemblages of the deep Northeast Atlantic: defining “Coral Gardens” to support future habitat mapping efforts. *ICES Journal of Marine Science* 70(3) 511-522.
- Cairns, S. D. & R. E. Chapman, 2001. Biogeographic affinities of the North Atlantic deep-water scleractinia. J. H. Martin Willison et al (eds) 2001. *Proceedings of the First International Symposium on Deep-Sea Corals*, Ecology Action Center and Nova Scotia Museum, Halifax, Nova Scotia, pp 30-57.

- Cairns, S. D. & F. M. Bayer, 2009. A genetic revision and phylogenetic analysis of the Primnoidae (Cnidaria: Octocorallia). *Smithsonian Contributions to Zoology*, 629. Smithsonian Institution Press: Washington DC USA. 79pp.
- Connell, J. H., 1978. Diversity in Tropical Rain Forests and Coral Reefs. *Science* 199: 1303-1310.
- Cordes, E. E., J. W. Nybakken & G. VanDykhuisen, 2001. Reproduction and growth of *Anthomastus ritteri* (Octocorallia: Alcyonacea) from Monterey Bay, California, USA. *Mar Biol* 138: 491-501.
- Etnoyer, P. & L. E. Morgan, 2005. Habitat-forming deep-sea corals in the Northeast Pacific Ocean. Freiwald A, Roberts JM (eds), 2005, *Cold-water Corals and Ecosystems*. Springer-Verlag Berlin Heidelberg, pp 331-343.
- Fadlallah, Y. H., 1983. Sexual Reproduction, Development and Larval Biology in Scleractinian Corals. *Coral Reefs* 2: 129-150.
- Flint, H. C., R. G. Waller & P. A. Tyler, 2007. Reproductive ecology of *Fungiacyathus marenzelleri* from 4100m depth in the northeast Pacific Ocean. *Mar Biol* 151: 843-849.
- Hall, V. R. & T. P. Hughes, 1996. Reproductive Strategies of Modular Organisms: Comparative Studies of Reef-Building Corals. *Ecology* 77(3) 950-963.
- Hoogenboom, M. O., S. R. Connolly & K. R. N. Anthony, 2008. Interactions between Morphological and Physiological Plasticity Optimize Energy Acquisition in Corals. *Ecology* 89: 1144-1154.
- Hwang, S. & J. Song, 2007. Reproductive biology and larval development of the temperate soft coral *Dendronephthya gigantean* (Alcyonacea: Nephtheidae). *Mar Biol* 152: 273-284.
- ICES. 2007. Report of the Working Group on Deep-water Ecology (WGDEC), 26-28 February 2007, ICES CM 2007/ACE:01 Ref. LRC. 61 pp. 45-46.
- Jackson, J. B. C., L. W. Buss & R. E. Cook, 1985. Population Biology and Evolution of Clonal Organisms. Yale University Press, New Haven and London.
- Jones, C. G., J. H. Lawton & M. Shachak, 1994. Organisms as ecosystem engineers. *OIKOS* 69: 373-386.
- Jones, G. P., G. R. Almany, G. R. Russ, P. F. Sale, R. S. Steneck, M. J. H. van Oppen & B. L. Willis, 2009. Larval retention and connectivity among population of corals and reef fish: history, advances and challenges. *Coral Reefs* 28: 307-325.
- Kahng, S. E., Y. Benayahu & H. R. Lasker, 2011. Sexual reproduction in octocorals. *Mar Ecol Prog Ser* 443: 265-283.
- Lacharite', L. & A. Metaxas, 2013. Early Life History of Deep-Water Gorgonian Corals May Limit Their Abundance. *PLoS ONE* 8(6): e65394. doi:10.1371/journal.pone.0065394.
- Lasker, H. R., D. A. Brazeau, J. Calderon, M. A. Coffroth, R. Coma & K. Kim, 1996. *In situ* Rates of Fertilization Among Broadcast Spawning Gorgonian Corals. *Biol. Bull.* 190: 45-55.

- Levinton, S. J., 1983a. The Latitudinal Compensation Hypothesis: Growth Data and a Model of Latitudinal Growth Differentiation Based Upon Energy Budgets. I. Interspecific Comparison of *Ophryotrocha* (Polychaeta: Dorvilleidae). *Biol. Bull.* 165: 686-698.
- Levinton, S. J. & R. K. Monahan, 1983b. The Latitudinal Compensation Hypothesis: Growth Data and a Model of Latitudinal Growth Differentiation Based Upon Energy Budgets. II. Interspecific Comparisons Between Subspecies of *Ophryotrocha puerilis* (Polychaeta: Dorvilleidae). *Biol. Bull.* 165: 699-707.
- Lumsden S. E, Hourigan T. F., Bruckner A. W. & Dorr G. (eds.) 2007. The State of Deep Coral Ecosystems of the United States. NOAA Technical Memorandum CRCP-3. Silver Spring MD.
- McFadden, C. S., 1986. Colony fission increases particle capture rates of a soft coral: advantages of being a small colony. *J. Exp. Mar. Biol. Ecol.* 103: 1-20.
- Mercier, A. & J.-F. Hamel, 2011. Contrasting reproductive strategies in three deep-sea octocorals from eastern Canada: *Primnoa resedaeformis*, *Keratoisis ornata*, and *Anthomastus grandiflorus*. *Coral Reefs* 30: 337-350.
- Metaxas, A. & J. Davis, 2005. Megafauna associated with assemblages of deep-water gorgonian corals in Northeast Channel, off Nova Scotia, Canada. *J. Mar. Biol. Ass. U. K.* 85: 1381-1390.
- Mistri, M, 1995. Gross morphometric relationships and growth in the Mediterranean gorgonian *Paramuricea clavata*. *Boll. Zool.* 62: 5-8.
- Morrison C. L., Baco A.R., Nizinski M.S., Coykendall D.K., Demopoulos A.W.J., Cho W. & Shank T., 2015. Population Connectivity of Dee-Sea Corals. In: Hourigan T.F., Etnoyer P.J., Cairns S.D. (eds) The State of Deep-Sea Coral and Sponge Ecosystems of the United States: 2015. NOAA Technical Memorandum X. NOAA, Silver Spring, p 12-1 – 12-30.
- Mortensen, P. B & L. Buhl-Mortensen, 2005. Morphology and growth of the deep-water gorgonians *Primnoa resedaeformis* and *Paragorgia arborea*. *Marine Biology* 147: 775-788.
- R Core Team (2017). R: A language and environment for statistical computing. R Foundation for Statistical Computing, Vienna, Austria. URL <https://www.R-project.org/>.
- Pechenik, J. A., 1999. On the advantages and disadvantages of larval stages in benthic marine invertebrate life cycles. *Mar Ecol Prog Ser* 177: 269-297.
- Pershing, A. J., M. A. Alexander, C. M. Hernandez, L. A. Kerr, A. Le Bris, K. E. Mills, J. A. Nye, N. R. Record, H. A. Scannell, J. D. Scott, G. D. Sherwood & A. C. Thomas, 2015. Slow adaptation in the face of rapid warming leads to collapse of the Gulf of Maine cod fishery. *Science* 350: 809-812.
- Ribes, M., R. Coma, S. Rossi & M. Micheli, 2007. Cycle of gonadal development in *Eunucella singularis* (Cnidaria: Octocorallia): trends in sexual reproduction in gorgonians. *Invertebrate Biology* 126(4): 307-317.
- Risk, M. J., J. M. Heikoop, M. G. Snow & R. Beukens, 2002. Lifespans and growth patterns of two deep-sea corals: *Primnoa resedaeformis* and *Desmophyllum cristagalli*. *Hydrobiologia* 471: 125-131.

- Roberts, J. M., A. J. Wheeler, A. Freiwald & S. D. Cairns, 2009. *Cold-Water Corals*. Cambridge University Press, Cambridge.
- Rowley, S. J., X. Pochon & L. Watling, 2015. Environmental influences on the Indo-Pacific octocoral *Isis hippuris* Linnaeus 1758 (Alcyonacea: Isididae): genetic fixation or phenotypic plasticity? *PeerJ* 3:e1128; DOI 10.7717/peerj.1128
- Sale, P. F., R. K. Cowen, B. S. Danilowicz, G. P. Jones, J. P. Kritzer, K. C. Lindeman, S. Planes, N. V. C. Polunin, G. R. Russ, Y. J. Sadovy & R. S. Steneck, 2005. Critical science gaps impede use of no-take fishery reserves. *TRENDS in Ecology and Evolution* 20: No. 2.
- Schluter, D., 2001. Ecology and the origin of species. *TRENDS in Ecology and Evolution* 16: 372-380.
- Sebens, K. P., 1984. Water flow and coral colony size: Interhabitat comparisons of the octocoral *Alcyonium siderium*. *Proc. Natl. Acad. Sci.* 81: 5473-5477.
- Sebens, K. P., 1987. The Ecology of Indeterminate Growth in Animals. *Ann. Rev. Ecol. Syst.* 18: 371-407.
- Shaish, L., A. Abelson & B. Rinkevich, 2007. How Plastic Can Phenotypic Plasticity Be? The Branching Coral *Stylophora pistillata* as a Model System. *PLoS ONE* 2(7): e644. doi:10.1371/journal.pone.0000644.
- Sherwood, O. A. & E. N. Edinger, 2009. Ages and growth rates of some deep-sea gorgonian and antipatharian corals of Newfoundland and Labrador. *Can. J. Fish. Aquas. Sci.* 66: 142-152.
- Sherwood, O. A., J. M. Heikoop, D. B. Scott, M. J. Risk, T. P. Guilderson & R. A. McKinney, 2005. Stable isotopic composition of deep-sea gorgonian corals *Primnoa* spp.: a new archive of surface processes. *Mar Ecol Prog Ser* 301: 135-148.
- Soetaert, K., C. Mohn, A. Rengstorf, A. Grehan & D. van Oevelen, 2016. Ecosystem engineering creates a direct nutritional link between 600-m deep cold-water coral mounds and surface productivity. *Sci. Rep.* 6, 35057; doi: 10.1038/srep35057
- Soong, K. & J. C. Lang, 1992. Reproductive Integration in Reef Corals. *Biol. Bull.* 183: 418-431.
- Stearns, S. C., 1989. The Evolutionary Significance of Phenotypic Plasticity. *BioScience* 39: 436-445.
- Sun, Z., J. F. Hamel & A. Mercier, 2010. Planulation periodicity, settlement preferences and growth of two deep-sea octocorals from the northwest Atlantic. *Mar. Ecol. Prog. Ser.* 410: 71-87.
- Thoma, J. N., E. Pante, M. R. Brugler & S. C. France, 2009. Deep-sea octocorals and antipatharians show no evidence of seamount-scale endemism in the NW Atlantic. *Mar. Ecol. Prog. Ser.* 397: 25-35.
- Thomas, A. C., A. J. Pershing, K. D. Friedland, J. A. Nye, K. E. Mills, M. A. Alexander, N. A. Record, R. Weatherbee & M. E. Henderson, 2017. Seasonal trends and phenology shifts in sea surface temperature on the North American northeastern continental shelf. *Elem. Sci. Anth.* 5: 48, DOI: <https://doi.org/10.1525/elementa.240>
- Tong, R., A. Purser, V. Unnithan & J. Guinan, 2012. Multivariate Statistical Analysis of Distribution of Deep-Water Gorgonian Corals in Relation to Seabed Topography on the Norwegian Margin. *PLoS ONE* 7(8): e43534. doi:10.1371/journal.pone.0043534.

- Tyler, P. A., A. Grant, S. L. Pain & J. D. Gage, 1982. Is annual reproduction in deep-sea echinoderms a response to variability in their environment? *Nature* 300: 747-750.
- van Hooijdonk, R., J. Maynard, J. Tamelander, J. Gove, G. Ahmadi, L. Raymundo, G. Williams, S. F. Heron & S. Planes, 2016. Local-scale projections of coral reef futures and implications of the Paris Agreement. *Sci. Rep.* 6, 39666; doi: 10.1038/srep39666.
- Watanabe, S., A. Metaxas, J. Sameoto & P. Lawton, 2009. Patterns in abundance and size of two deep-water gorgonian octocorals, in relation to depth and substrate features off Nova Scotia. *Deep-Sea Research I* 56: 2235-2248.
- Watling, L. & P. J. Auster, 2005. Distribution of deep-water Alcyonacea off the Northeast Coast of the United States. *Cold-Water Corals and Ecosystems*, Springer-Verlag Berlin Heidelberg, pp 279-296.
- Watling, L., S. C. France, E. Pante & A. Simpson, 2011. Biology of Deep-Water Octocorals. *Advances in Marine Biology* 60: 41-122.
- Waller, R. G., P. A. Tyler & J. D. Gage, 2002. Reproductive ecology of the deep-sea scleractinian coral *Fungiacyathus marenzelleri* (Vaughan, 1906) in the northeast Atlantic Ocean. *Coral Reefs* 21: 325-331.
- Waller, R. G. & P. A. Tyler, 2005. The reproductive biology of two deep-water, reef-building scleractinians from the NE Atlantic Ocean. *Coral Reefs* 24: 514-522.
- Waller, R. G., L. Watling, P. Auster & T. Shank, 2007. Anthropogenic impacts on the Corner Rise seamounts, north-west Atlantic Ocean. *J. Mar. Biol. Ass.* 87: 1075-1076.
- Waller, R. G., R. P. Stone, J. Johnstone & J. Mondragon, 2014. Sexual Reproduction and Seasonality of the Alaskan Red Tree Coral, *Primnoa pacifica*. *PLoS ONE* 9(4): e90893. doi:10.1371/journal.pone.0090893.
- West-Eberhard, M. J., 2005. Developmental plasticity and the origin of species differences. *PNAS* 102: 6543-6549.
- Yesson, C., M. L. Taylor, D. P. Tittensor, A. J. Davies, J. Guinotte, A. Baco, J. Black, J. M. Hall-Spencer & A. D. Rogers, 2012. Global habitat suitability of cold-water octocorals. *Journal of Biogeography* 39: 1278-1292.

APPENDIX. ADDITIONAL FIGURES AND DATA FROM 2017 CRUISE

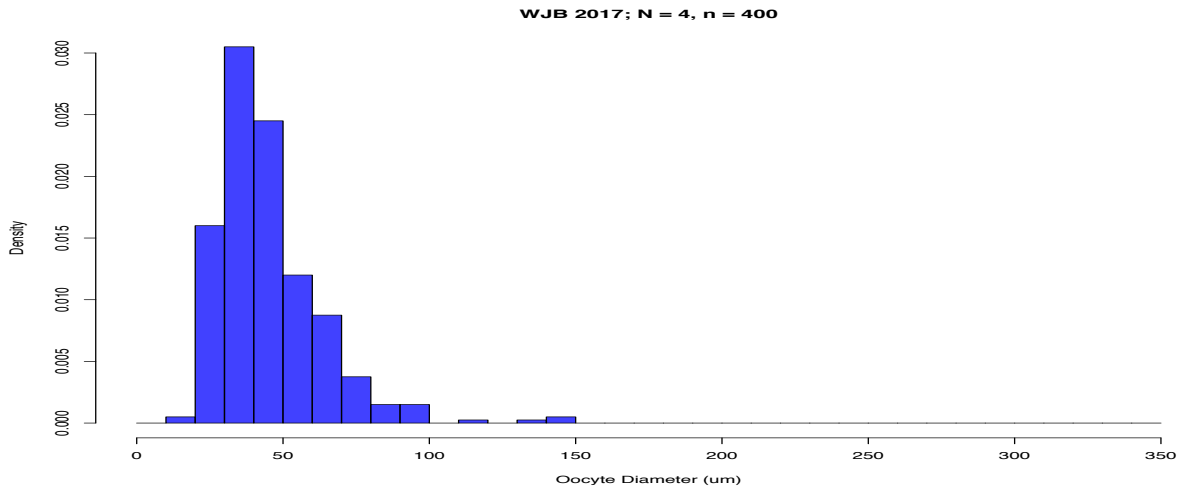


Figure 19. Oocyte size distribution of *P. placomus* from samples collected in June 2017 from the Western Jordan Basin (WJB). These data are investigated further in the section “Seasonal Reproductive Variability”.

Oocyte diameter frequency distributions from 2017 are shown in **Figure 19** and include sampled subpopulations from Western Jordan Basin (WJB), Nygren-Heezen InterCanyon (NHI), and Corsair Canyon (CC). The same Dunn *post hoc* test was run showing statistical significance ($p < 0.05$), when making a pairwise comparison between height distributions.

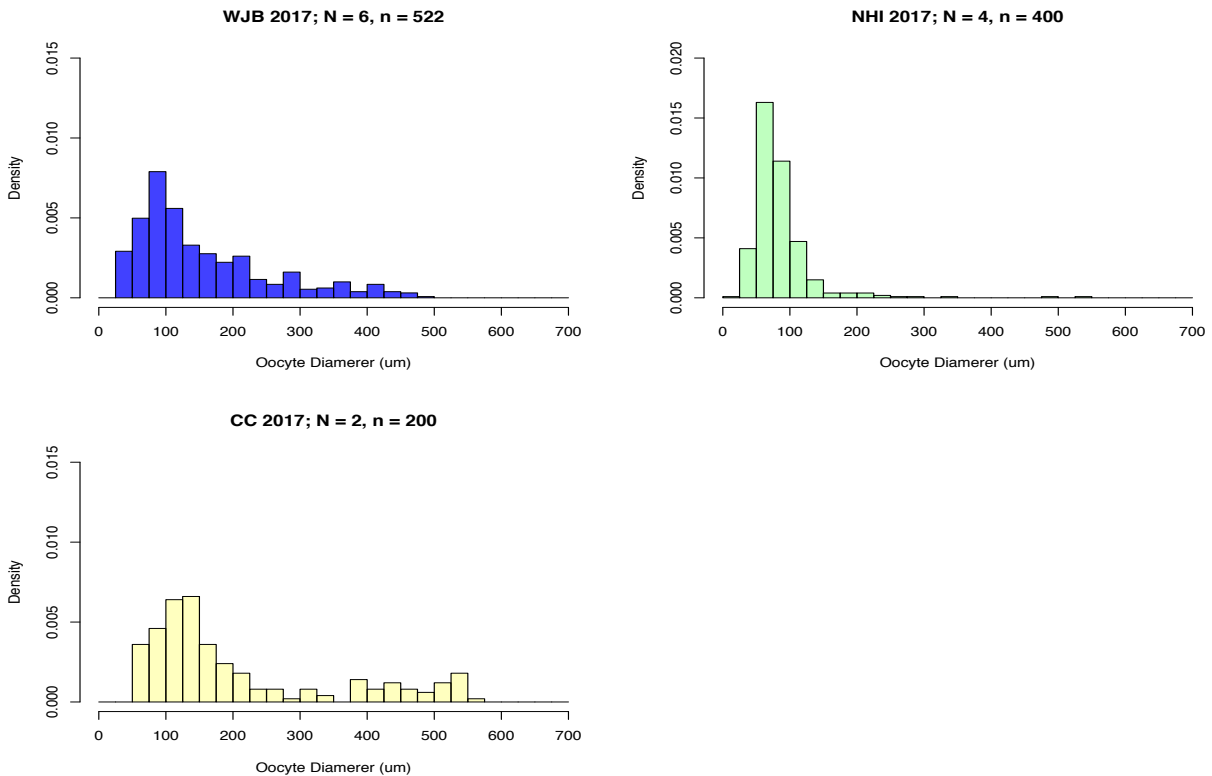


Figure 20. Oocyte size distribution of *P. resedaeformis* from samples collected in June 2017 from the Western Jordan Basin (WJB), Nygren-Heezen InterCanyon (NHI), and Corsair Canyon (CC). These data are investigated further in the section “Seasonal Reproductive Variability”.

BIOGRAPHY OF THE AUTHOR

C. Tyler Fountain was born on September 6, 1990 and raised in Columbus, Ohio. He graduated from Upper Arlington High School in 2009, where he pursued various arts, sciences, and athletics. These interests followed him while attending Capital University, from which he graduated, in 2013, with a Bachelor's degree in Biology. What does one do with a degree in biology? you may wonder. The answer lies within the title, they study life, and that is exactly what he has done ever since. These studies have taken him to various locations throughout the Caribbean, Andros Island being a particularly memorable one, and left him knocking at the door for graduate school at the University of Maine. After receiving his degree Tyler has no idea what he will be doing next, but that is ok, he will remain flexible and adapt to life as it comes his way. A PhD would be nice though... You can't really be a professor without one of those. Tyler is a candidate for the Master of Science degree in Marine Biology from the University of Maine in May 2018.